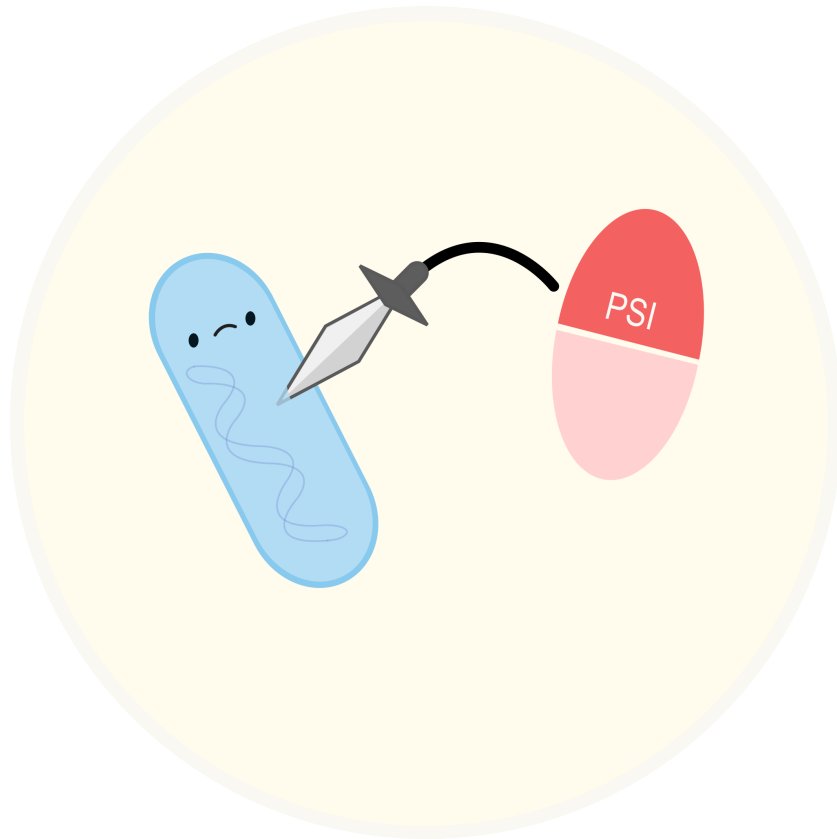


Understanding the Impact of Diverse Antibiotics on Gut Bacteria Survival



MASTER THESIS IN BIOTECHNOLOGY

MICAEL LIBERTELLA

SUPERVISOR: *PROFESSOR CAMILLE GOEMANS*

INTERNAL SUPERVISOR: *PROFESSOR JEPPE LUND NIELSEN*

EPFL UNIVERSITY - AALBORG UNIVERSITY

31/05/2025



AALBORG UNIVERSITET
STUDENTERRAPPORT

Department of Chemistry and Bioscience
Aalborg University
Biotechnology
Fredrik Bajers Vej 7H
9220 Aalborg Ø

Title: Understanding the Impact of
Diverse Antibiotics on Gut Microbiota

ECTS:

60 ECTS **Semester:**
9-10th. semester

Project period:

Spring and autumn semester 2025

Internship:

EPFL University

- Lab of Drug and Microbiota Interactions

Supervisor:

Camille Goemans

Internal Supervisor:

Jeppe Lund Nielsen

I would like to thank Camille Goemans for her guidance and tutorage throughout the months. Thanks to Jeppe Lund Nielsen for his help as the internal supervisor. I would also like to thank my family for the endless support, and Rachel Gianna Scalzetti, with whom I share my heart and future, for her constant encouragement and motivation.

No. of pages: 78

Abstract:

The human gut microbiota is composed of different commensal bacteria, fungi and viruses, essential for the host's health: commonly prescribed antibiotics alter its composition, leading to dysbiosis. Previous studies have shown that bacteriostatic antibiotics, thought to be better for the health of gut bacteria, have bactericidal activity towards some strains. This study aims to investigate in more detail the diverse staticidal effect of an array of different antibiotics against commensal bacteria commonly found in the gut microbiota. Through a high-throughput measurement, Minimum Inhibitory concentration (MIC) values are measured for bacteria of interest, not available on public databases, and needed to study the effect of various antibiotics on specific strains through a survival assay. This study concludes that the majority of previously defined bacteriostatic antibiotics actually show bactericidal effects.

Preface

Aalborg University, 31/05/2025

Micael Libertella

mliber23@student.aau.dk,

Micael.libertella@gmail.com

Abbreviations

Abbreviation - Meaning

- AUC – Area Under the Curve
- AMX – Amoxicillin
- AZM – Azythromycin
- CFU – Colony Forming Unit
- CHL – Chloramphenicol
- CIP – Ciprofloxacin
- CLI – Clindamycin
- CLR – Clarythromycin
- CRO – Ceftriaxone
- CTX – Cefotaxime
- DNA – Deoxyribonucleic Acid
- DOX – Doxycycline
- DMSO – Dimethyl Sulfoxide
- ERY – Erythromycin
- GAT – Gatifloxacin
- GI – Gastro-Intestinal
- IL - Interleukin
- ILCs – Innate Lymphoid Cells
- Ig – Immunoglobulin
- LNZ - Linezolid
- MBC – Minimum Bactericidal Concentration
- MEM – Meropenem
- MIC – Minimum Inhibitory Concentration
- mGAM – modified Gifu Anaerobic Media
- mRNA – messenger RNA
- MTZ – Metronidazole
- MXF – Moxifloxacin
- NAG – N-AcetylGlucosamine

- NAM – N-AcetylMuramic Acid
- OFX - Ofloxacin
- OD – Optical Density
- OM – Outer Membrane
- PBS – Phosphate-buffered saline
- PBP – Penicillin Binding Protein
- PTC – Peptidyl Transfarase Center
- PSI – Protein Synthesis Inhibitors
- RNA – Ribonucleic Acid
- rRNA – ribosomal RNA
- SCFA – Short Chain Fatty Acids
- TEC – Teicoplanin
- TET – Tetracycline
- TIG – Tigecycline
- Tregs – Regulatory T cells
- tRNA – transfer RNA
- VAN – Vancomycin

Contents

Preface	i
Abbreviation	ii
1 Introduction	1
1.1 Human Gut Microbiota	2
1.1.1 Functions of the Gut Microbiota	3
1.2 Dysbiosis	5
1.3 Antibiotics	7
1.4 Classification of antibiotics based on their mechanism of action	7
1.4.1 Cell Wall inhibition	8
1.4.2 DNA Replication Inhibition	10
1.4.3 Protein Synthesis Inhibitors	11
1.4.4 Nitroimidazole	14
2 Problem statement	15
3 Experimental Theory	17
3.1 MIC and MBC	17
3.2 Survival assay	18
3.3 Optical Density Measurements	19
4 Experimental Overview	20
5 Materials & Methods	22
5.1 Materials and Apparatus	22
6 Methods	24
6.1 MIC Drug Plates preparation	24
6.2 MIC analysis	27
6.2.1 Script for MIC breakpoint detection	28
6.3 Colony Forming Units and detection time counting	29

6.3.1	Spotting assay	30
6.3.2	Detection time	30
6.4	Survival Assay through detection time count	31
6.5	Survival Assay through spotting assay	33
6.6	Phylogenic tree	34
7	Results	35
7.1	MIC Measurement	35
7.2	CFU concentration to detection time relationship	38
7.3	Survival Assay through detection time counting	40
7.4	Survival assay with spotting	43
8	Discussion	45
8.1	MIC measurements	45
8.2	Survival Assay through detection time counting	47
8.3	Survival Assay through Spotting	47
9	Conclusion	49
10	Reflection	50
	Bibliography	51
11	Appendix	59
11.1	Calibration curves	59

Introduction

1

The human gut microbiota is a community of commensal microbes that populate our Gastrointestinal (GI) tract; a healthy gut microbiota is a diverse one.

The gut microbiota is fundamental to maintain the hosts' health; it influences the immune system, metabolism and digestion (e.g. with the production of essential molecules like vitamins or the production of Short Chain Fatty Acids (SCFAs)), and protects our gut against pathogens and more.

Studies have also shown that the gut microbiota influences and is influenced in a bi-directional way in what is called the "gut-brain axis" through the production of neurotransmitters such as serotonin and dopamine, influencing mood, stress response, cognitive function, and hunger cues [Gomaa, 2020; Marano et al., 2023].

It is widely known that alteration to the composition of the microbiota, defined as dysbiosis, leads to health-related issues that can have long-lasting effects. Reduced diversity can lead to the loss of commensal beneficial microbes, reducing the competition and allowing the spread of pathogens and/or reduction of previously described benefits derived from the diverse microbiota.

Although many factors can induce dysbiosis, antibiotics, being one of the most commonly known and used medications, are of particular interest, with multiple studies showing a direct correlation with antibiotic consumption and dysbiosis. Intake of these compounds, even in low dosage from the environment and food, or sub-therapeutic doses of antibiotics, influences the host's gut microbiota [Konstantinidis et al., 2020; Petersen and Round, 2014]. The effects of antibiotics on the bacteria present in the gut are still not well characterised, with recent studies showing previously classified bacteriostatic antibiotics, such as macrolides and tetracyclines, having bactericidal effects *in vitro* on the indigenous commensal bacteria of our gut [Maier et al., 2021].

1.1 Human Gut Microbiota

"Gut microbiota" refers to the ensemble of microbes, such as bacteria, but also fungi, archaeobacteria, and viruses, residing in the GI tract (**figure 1.1**). The gut microbiota is defined by its abundance and diversity in bacterial species, which are highly different even between genetically related individuals. The difference in composition of the microbiota is due to multiple factors, primarily diet, age, gender, habits (i.e smoking or exercise), infections, geographical impacts (i.e dietary patterns, climate, food availability, access to clean water), and medication intake [Slingerland et al., 2017; Konstantinidis et al., 2020; Clemente et al., 2012; Hou et al., 2022].

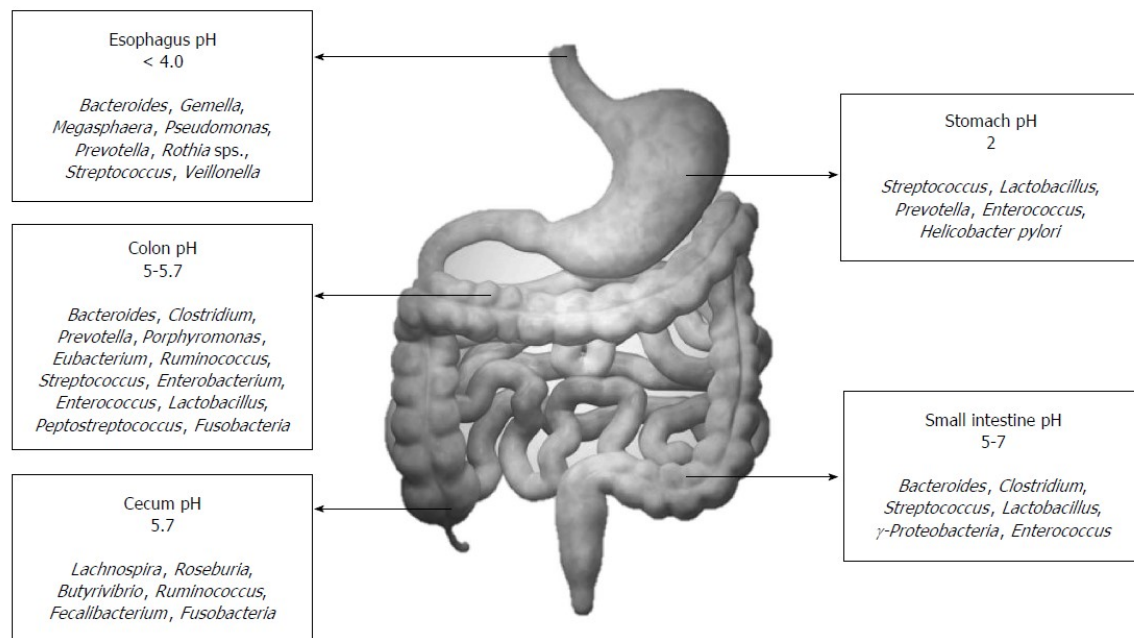


Figure 1.1. Example of distribution of the gut microbiota depending on the location within the GI tract [Jandhyala et al., 2015]

Microbial composition varies depending on the section of the GI tract. Having 99% of the microbial composition comprised of around 30-40 different species [Shapira, 2016; Alonso and Guarner, 2013; Hou et al., 2022]. Although the composition is significantly diverse in different hosts, 90% of them belong to the phyla Bacteroidetes and Firmicutes [Konstantinidis et al., 2020].

1.1.1 Functions of the Gut Microbiota

The gut microbiota is involved in multiple functions, such as nutrient metabolism, protection of our gut against pathogens, immunomodulation, and its relation to the "gut-brain axis" [Gomaa, 2020; Marano et al., 2023].

1.1.1.1 Nutrient metabolism

Complex carbohydrates, such as dietary fibers introduced in our nutrition that cannot be metabolised, are directed to our colon, where some bacteria can use them as nutrients [Jandhyala et al., 2015].

Complex carbohydrates are fermented into Short Chain Fatty Acids (SCFAs), which are generally absorbed by the colonic lining cells and used as energy by oxidising these molecules [Shin et al., 2023]. The most important SCFAs are acetate, propionate, and butyrate, which are distributed generally in a 60:20:20 proportion susceptible to variation through diet. Acetate is involved in energy production and lipid synthesis; propionate is involved in glucose production in the small intestine and liver; and butyrate is used as an energy source by colonic lining cells (**figure 1.2**). [Shin et al., 2023; Donohoe et al., 2011; Corrêa-Oliveira et al., 2016; Jandhyala et al., 2015]. Butyrate has anti-inflammatory properties and helps maintain the gut barrier integrity by promoting mucus production [Jandhyala et al., 2015; Pant et al., 2023].

The gut microbiota is also involved in the production of essential vitamins like vitamin K and B such as Biotin (Vitamin B7), thiamine, cobalamin, riboflavin, nicotinic and pantothenic acids [LeBlanc et al., 2013].

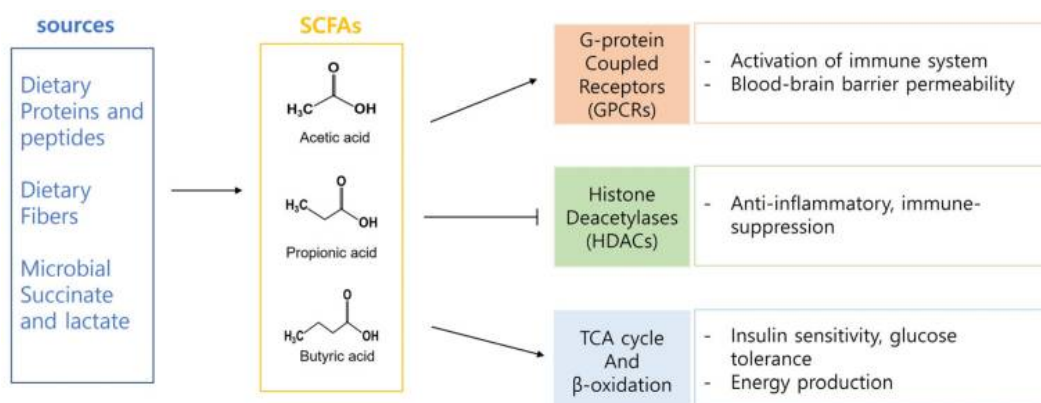


Figure 1.2. Functions of SCFAs in the gut. [Shin et al., 2023]

1.1.1.2 Protection against pathogens

The gut microbiota is present on both the large and small intestines in more micro-aerobic conditions, or on the outer mucus layer, where it can be exposed to food sources and grow in anaerobic conditions. The complex community formed in the gut generally disallows the growth of pathogens through substrate competition by occupying and utilising the majority of the space and food resources, disincentivising the growth of microbes outside of the already established population ecology [Kennedy and Chang, 2020; Horrocks et al., 2023]

In addition to nutrient competition between our microbiota and pathogens, the production of bacteriocins (peptidic toxins produced by bacteria) and of inhibitory metabolites, such as some SCFAs that can also inhibit the growth of some bacteria, and the presence of bacteriophages, contribute to the protection of the host [Horrocks et al., 2023].

1.1.1.3 Immunomodulation

The gut microbiota influences the immune system by promoting tolerance to beneficial microbes while defending against pathogens, as stated beforehand. With the production of antigens, it also supports the development of Gut-Associated Lymphoid Tissues and helps to produce immune cells like regulatory T cells (Tregs), plasma B cells, which produce IgA antibodies, innate lymphoid cells (ILCs), and macrophages. Gut bacteria can stimulate the production of anti-inflammatory molecules (cytokines, small proteins with a cell signaling function) like IL-10 and barrier-protecting like IL-22. SCFAs from bacterial fermentation promote Treg development, while microbial metabolites regulate ILCs and activate dendritic cells to enhance IgA production, helping to maintain immune homeostasis and prevent harmful infections. [Jandhyala et al., 2015; Hou et al., 2022]

1.1.1.4 Gut-brain axis

The gut microbiota and the brain can influence and communicate in a bi-directional way in what is called the gut-brain axis. Key functions of this axis include regulating gut motility, contraction and relaxation of muscles for food movement, intestinal permeability, endocrine signals through hormones, and immune signaling through cytokines. Through the production of neurotransmitters such as serotonin, Gamma-Amino Butyric Acid and dopamine precursors, commensal bacteria can influence our mood, stress response, and cognitive function. Changes in the microbiota, due to various external factors, or habits such as diets, are linked to neurodevelopmental and mood disorders, schizophrenia, anxiety, and Alzheimer's disease.

The production of SCFAs also contributes to the integrity of the blood-brain barrier, a semi-permeable barrier separating the circulating blood from the central nervous system, which prevents harmful substances from entering the brain. SCFA inside the endothelial cells of the brain, upregulate the expression of tight junction proteins, molecules that form complexes at the junctions between adjacent epithelial and endothelial cells[Hou et al., 2022; Gomaa, 2020; Marano et al., 2023].

1.2 Dysbiosis

As previously defined, dysbiosis is the imbalance or disruption of the ecology present in our gut, due to its variation in diversity and abundance, leading to a change in metabolic activities and distribution of bacteria with the loss of beneficial commensals. Loss of diversity is especially problematic for the expansion of pathobionts, which are native bacteria that assume pathogenicity after changes environmental changes or in the microbiome composition. Sudden expansion and prevalence of the pathobionts in microbiota can lead to inflammation and pathology (**figure 1.3**) [Petersen and Round, 2014; Jandhyala et al., 2015].

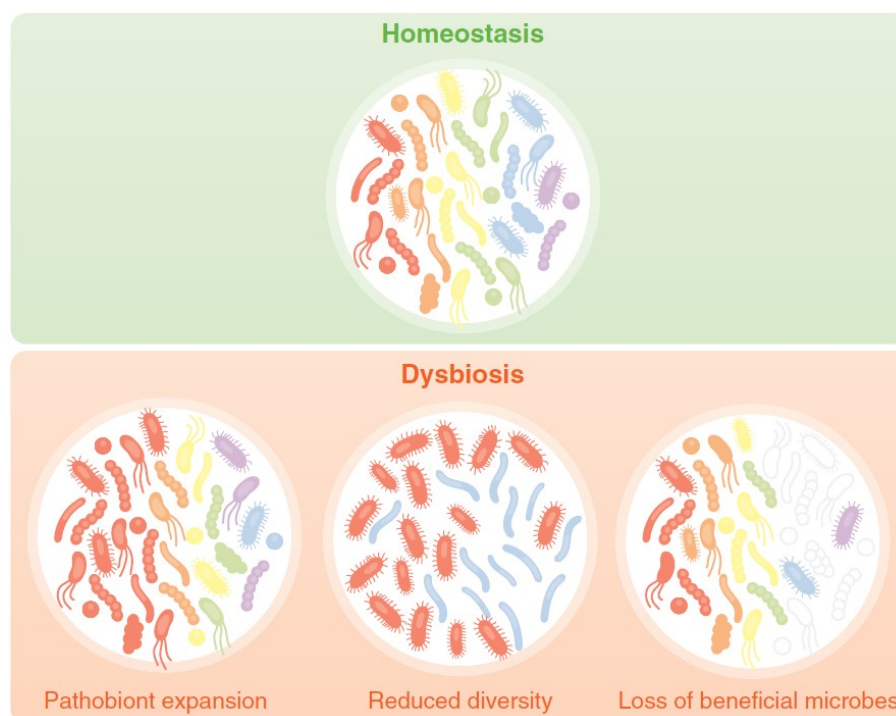


Figure 1.3. Lack of diversity of commensal bacteria may lead to the expansion of pathogenic bacteria or pathobionts, bacteria that will develop pathogenic traits [Petersen and Round, 2014].

Dysbiosis has been associated with numerous conditions such as obesity, autism, diabetes, inflammatory bowel disease, non-alcoholic and alcoholic fatty liver disease, cardiovascular diseases, and chronic kidney disease. It can also lead to disruption in nutrient metabolism and increase permeability of the gut, leading to what is generally defined as "leaky-gut", easing the penetration of pathogens and bacterial secondary metabolites in the inner mucose layers of the intestines. Dysbiosis can lead to many more diseases, as listed in (**figure 1.4**) [Jandhyala et al., 2015; DeGruttola et al., 2016; Hou et al., 2022].

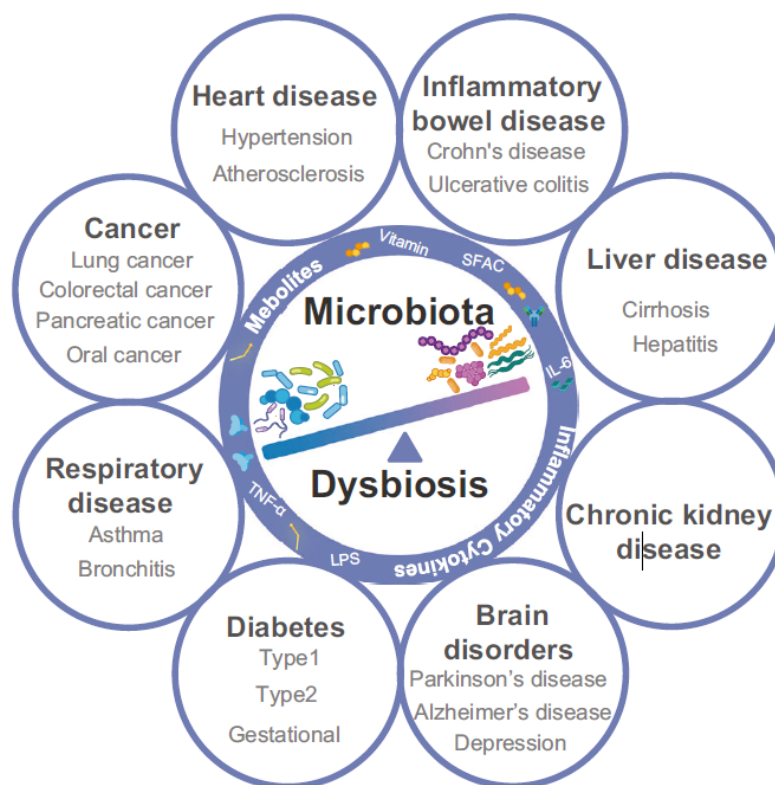


Figure 1.4. Effects of dysbiosis [Hou et al., 2022]; a serious of health related issues that may appear once there is shift in the microbiome composition regarding abundancy and diversity of the gut microbiota.

Although many factors can induce dysbiosis, the intake of antibiotics shows a direct correlation to the modification of the host's gut microbiota [Konstantinidis et al., 2020; Petersen and Round, 2014]. Previous studies have also shown that commonly defined bacteriostatic antibiotics such as clindamycin, which should theoretically affect less the gut microbiota, had a more long-lasting and serious impact on its diversity[Zaura et al., 2015].

1.3 Antibiotics

Antibiotics are a type of compound that targets bacteria by forestalling bacterial growth or targeting cellular functions or processes within the cell to kill or inhibit it. Antibiotics are generally classified as bactericidal, which means that they kill bacteria, or as bacteriostatic, which means that they inhibit growth [Nemeth et al., 2014; Pankey and Sabath, 2004a]. To study antibiotic activity, Minimum Inhibitory Concentration (MIC), or the lowest concentration that inhibits the visible growth of bacteria, and the Minimum Bactericidal Concentration (MBC), or minimum concentration that kills bacteria, are used [Pankey and Sabath, 2004a]. An antibiotic is defined as bacteriostatic if the proportion between MBC to MIC is greater than 4, and bactericidal if it is less. The efficacy of an antibiotic is influenced by many conditions such as the type of bacteria, the quantity of bacteria, and the site of infection. Thus, in different conditions, and depending on the type of bacteria, a bacteriostatic antibiotic can exhibit bactericidal effects [Nemeth et al., 2014; Pankey and Sabath, 2004a].

1.4 Classification of antibiotics based on their mechanism of action

Antibiotics can be classified based on their interaction and interference with the targeted prokaryotic cell. Three main categories can be defined by the synthesis inhibition of cell walls, nucleic acids, and proteins. [Kapoor et al., 2017]

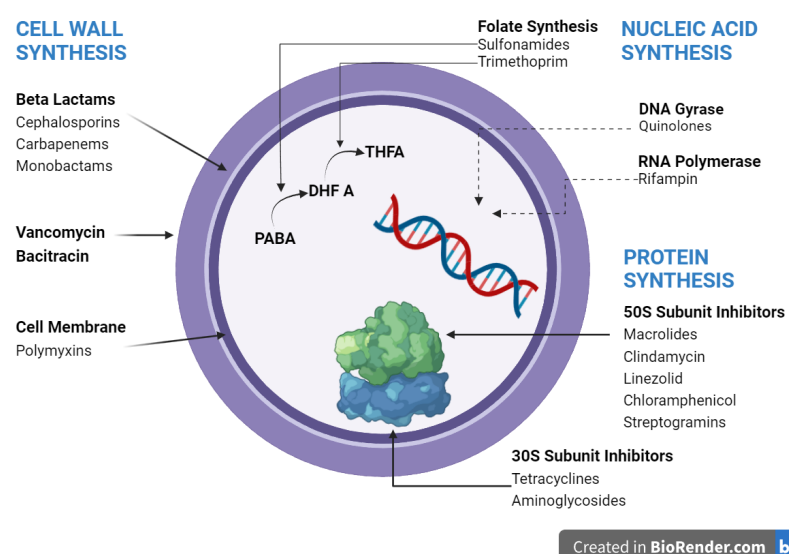


Figure 1.5. Types of antibiotics based on their inhibitions target with some examples of families. Adapted from [Kapoor et al., 2017] through BioRender.com (2024).

1.4.1 Cell Wall inhibition

The cell wall is formed mainly by peptidoglycan layers, polysaccharides, consisting of β -(1,4) glycosidic bond linking N-acetylglucosamine (NAG) and N-acetylmuramic acid (NAM) residues alternating each other. Attached to the NAM, an oligopeptide of 3-5 residues is found that can cross-link between other peptidoglycan strands [Madigan et al., 2014]. More in detail, there is a cross-linking of the D-alanyl-D-alanine with glycine residues of the Penicillin Binding Protein (PBP), this interaction helps strengthen the lattice, and providing structural integrity [Reynolds, 1989b].

Beta-lactams are a group of antibiotics whose mechanism of action focuses on inhibiting bacterial cell wall synthesis by targeting penicillin-binding proteins (PBPs), as illustrated in **figure 1.6-A**. It is supposed that the lactamic ring, mimics and competes with the D-alanyl-D-alanine for linking with the PBP, effectively diminishing the available concentration for the synthesis of new peptidoglycan, disrupting the layers of the lattice and leading to the lysis of bacteria. Beta-lactams work on both Gram-positive and negative bacteria, with their efficiency depending on the molecule and the targeted bacterial strain [Kos et al., 2008].

Both penicillins (such as amoxicillin), and cephalosporins (such as ceftriaxone and cefotaxime) act by binding irreversibly to the PBP leading to a weakened wall that triggers the lysis of the cell. These antibiotics thus have a bactericidal effect and are effective against Gram-positive bacteria and some Gram-negative [KONG et al., 2010; Bush and Bradford, 2016; Kos et al., 2008].

Carbapenems are a subclass of bactericidal beta-lactam antibiotics that exhibit broad-spectrum activity due to their high affinity for multiple penicillin-binding proteins with the same mechanism of action as penicillins. Conversely to other beta-lactams, these compounds are able to target both Gram-positive bacteria and Gram-negative, given their small size and ability to penetrate the outer membrane through porins [Papp-Wallace et al., 2011; Saikia and Chetia, 2024].

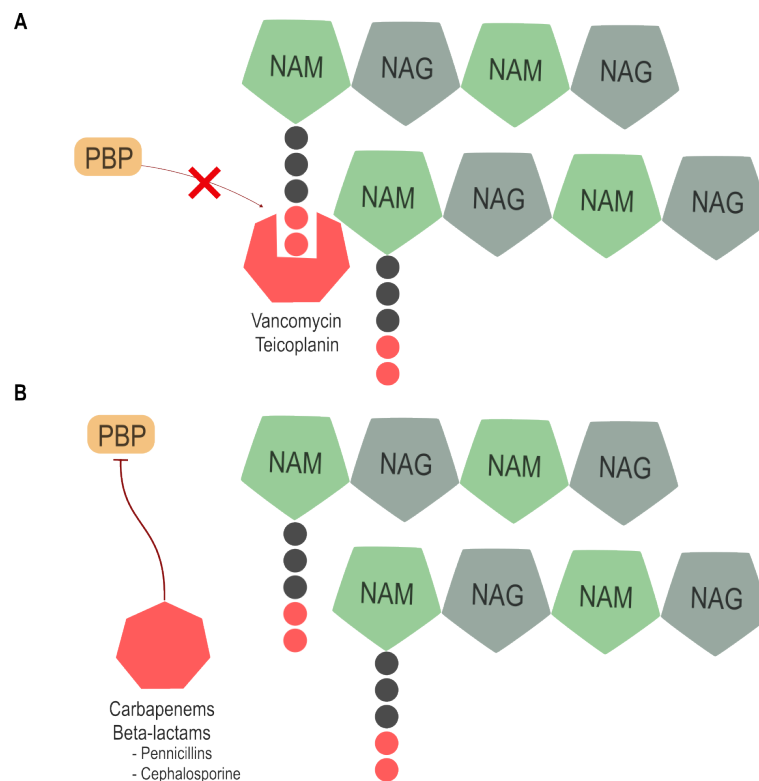


Figure 1.6. Mechanism of action of Cell wall synthesis inhibitors. **A.** Glycopeptides such as vancomycin and teicoplanin bind directly to the D-Ala-D-ala portion of the peptide sidechain of the peptidoglycan subunit, impeding the binding of the PBP, competing for the substrate **B.** Beta-lactams antibiotics such as amoxicillin (penicillin group), ceftriaxone and cefotaxime (cephalosporin group), and meropenem (carbapenem group), directly bind and inhibit PBP.

Glycopeptides, such as vancomycin and teicoplanin, are a group of antibiotics defined as bactericidal that share the same mechanism of action, inhibiting bacterial cell wall synthesis by binding to the D-Ala-D-Ala terminal of peptidoglycan precursors, as illustrated in **figure 1.6-B**. These compounds, as previously explained in section 1.4.1, physically block peptidoglycan cross-linking, therefore competing with the PBP for the substrate preventing proper cell wall formation, and resulting in cell death due to osmosis or leakage of intracellular components. This class of antibiotics is very effective against Gram-positive bacteria, but ineffective against Gram-negative given the nature of their outer layer and the size of the compound [Kapoor et al., 2017; Donadio and Sosio, 2014; Patel et al., 2017; Reynolds, 1989a].

1.4.2 DNA Replication Inhibition

Most common inhibitors for DNA replications are able to interact with DNA Gyrase. These proteins are formed by two subunits A, which introduce a nick into the sugar-phosphate backbone of the DNA and resealing it, and two B subunits which introduce a negative supercoil, to alleviate the positive supercoiling given by the enzyme helicase [Reece et al., 1991; Collin et al., 2011].

Fluoroquinolones are a group of antibiotics whose mechanism of action focuses on inhibiting bacterial DNA replication by targeting DNA gyrase (Topoisomerase II in Gram-negative bacteria and IV in Gram-positive bacteria), which are absent in mammalian cells. These compounds bind to the subunit A of the DNA-gyrase enzyme complex or topoisomerase IV in Gram-positive, and stabilize the complex after the formation of the nick, essential for relieving supercoiling tension during DNA replication. Stabilizing the DNA break, and preventing relegation, will lead to double-stranded DNA fragmentation and cell death, thus being defined as bactericidal.

Due to their hydrophilic and lipophilic properties, fluoroquinolones such as ciprofloxacin, gatifloxacin, moxifloxacin, and ofloxacin can penetrate bacterial cells and exhibit broad-spectrum activity against both Gram-positive and Gram-negative bacteria, and disrupt DNA replication and transcription [Blondeau, 2004; Kapoor et al., 2017; Higgins et al., 2003].

Mammalian cells present a topoisomerase II, which has a low affinity to Fluoroquinolones. Consequently this category of antibiotics is selective towards bacteria only [Aldred et al., 2014; Higgins et al., 2003; Yoneyama and Katsumata, 2006].

1.4.3 Protein Synthesis Inhibitors

Protein Synthesis Inhibitors are a category of drugs that affects the process of protein production. This family of antibiotics works on the two ribonucleoprotein subunits 30s and 50s. Antibiotics in this family act during the initiation, elongation, and termination of protein synthesis.

1.4.3.1 PSIs - 30s

Tetracyclines are a group of antibiotics whose mechanism of action focuses on reversibly binding to the A-site of the 30s ribosomal subunit, as illustrated in **figure 1.7**. The inhibition of the protein synthesis is given by the competition of these types of compounds against the aminoacyl-tRNA for the binding site with binding strength varying on the affinity of the ligating antibiotic. The lipophilic nature of these molecules allows the passage by passive diffusion through various membranes of lipidic nature to reach its target.

Therefore, tetracyclines keep bacteria in a non-growing phase, impeding the production of fundamental proteins, characterising it as a bacteriostatic antibiotic [National Center for Biotechnology Information, 2025a; Patel and Parmar, 2023; Chopra and Roberts, 2001].

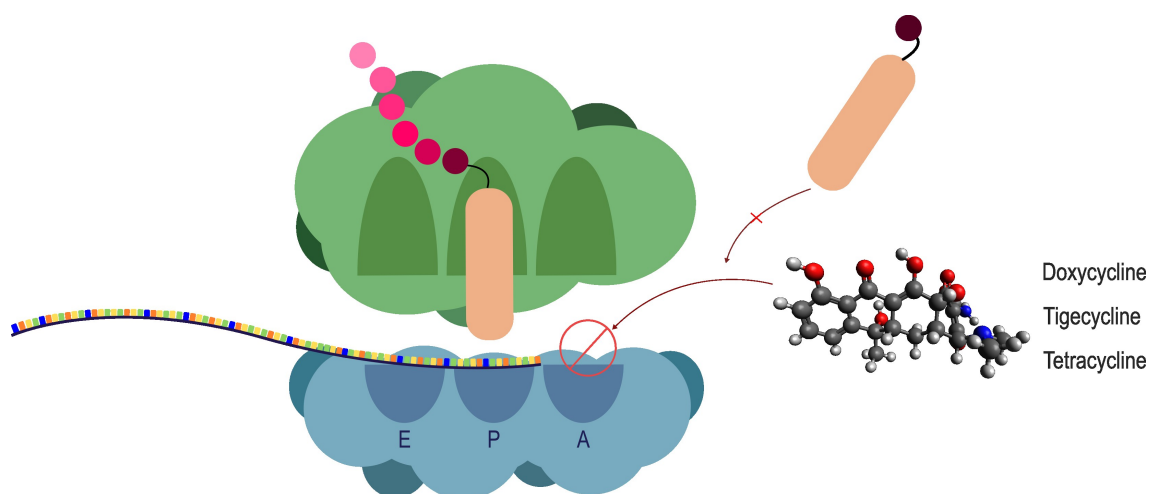


Figure 1.7. Tetracyclines reversibly bind with different strengths depending on the affinity of the compound interacting on the A-site of the 30s ribosomal subunit, keeping the ribosome on a constant elongation phase

Doxycycline is a second-generation tetracycline, currently used for treating various infections of bacteria both Gram-positive and negative, on both aerobes and anaerobes. Being in the same family as tetracycline, it possesses similar structure and pharmacodynamics and is characterized by its highly lipophilic nature and stronger affinity towards the ribosomal A-site, avoiding some types of resistance towards tetracycline [National Center for Biotechnology Information, 2025a; Patel and Parmar, 2023].

Lastly, tigecycline, is a third-generation tetracycline or first-generation glycylcycline, with a similar structure to tetracyclines and with a 5 fold stronger affinity to the binding site, making it more effective against bacteria presenting tetracycline resistance [Yaghoubi et al., 2022].

1.4.3.2 PSIs - 50s

Macrolides are a group of antibiotics whose mechanism of action focuses on binding to the 50S ribosomal subunit, as illustrated in **figure1.8-A**. These classes of compounds act by binding to the Peptidyl-Transferase Center (PTC), with different affinity depending on the antibiotic, blocking the peptide exit tunnel, and preventing elongation. This leads to a premature dissociation of the growing peptide chain. Due to their relatively large and lipophilic structure, macrolides can easily penetrate host cells, making them particularly effective against intracellular pathogens. As a result, macrolides such as azithromycin, erythromycin, and clarithromycin inhibit protein synthesis resulting in a bacteriostatic effect. These macrolides target more effectively Gram-positive bacteria, with a slight effect on Gram-negative and anaerobic depending on the species. [Patel and Hashmi, 2023; Van Bambeke and Tulkens, 2001; Schlünzen et al., 2001].

Linezolid is defined as a bacteriostatic antibiotic from the oxazolidinones class. This antibiotic binds to the 50s ribosomal subunit; more specifically, it is thought to bind to the 23s subunit, on the PTC, inhibiting the formation of the 70s ribosome initiation complex, as seen in **figure1.8-C**. [Diekema and Jones, 2000; Azzouz and Preuss, 2024]. Linezolid can be used on both Gram-positive and negative bacteria with claims that its *in vitro* activity against Gram-negative and anaerobic bacteria is not considered effective [National Center for Biotechnology Information, 2025d].

Clindamycin is an antibiotic from the Lincosamides class, which can target some Gram-positive aerobic bacteria and both Gram-positive and Gram-negative anaerobic bacteria. This compound binds to the 50s ribosomal subunit, with the PTC as its binding site, affecting the peptide chain formation, as shown in **figure 1.8-B**, thanks to its structure resembling a peptide-loaded tRNA. This results in the blocking ribosomal translocation and stalling it into the elongation phase with the drop out of a premature peptidyl-tRNA, resulting in a bacteriostatic effect [Murphy et al., 2024; National Center for Biotechnology Information, 2025c; Spížek and Řezanka, 2017].

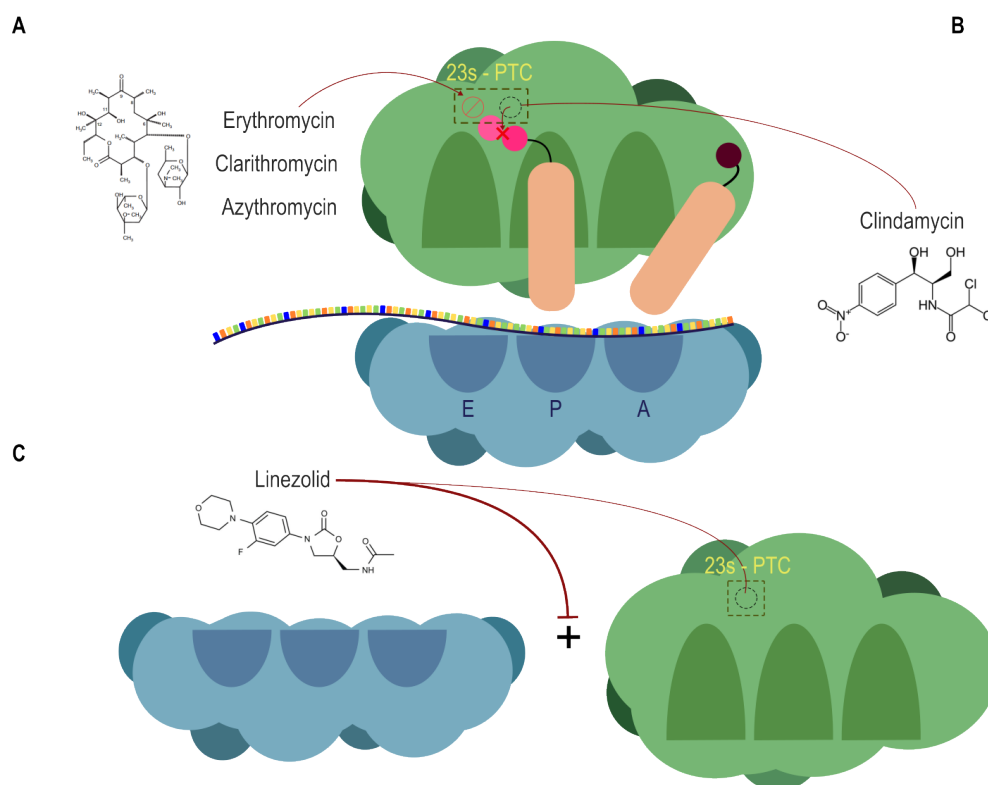


Figure 1.8. Mechanism of action of Protein synthesis inhibitors targeting the 50s subunit. **A.** Macrolides bind to the 23s, to the PTC, with different binding affinity where Azithromycin > Clarithromycin > Erythromycin. Macrolides binding to the 23s cause a blockage of the exit tunnel for the peptide in formation, halting the protein synthesis during the elongation phase. **B.** Clindamycin competes for the same binding site, but impedes the creation of a peptidic bond, halting the synthesis. **C.** Linezolid, still attaches to the same site but halts the formation of the 70s ribosomal complex, stopping the synthesis from the beginning.

Chloramphenicol is a compound in the amphenicol class, defined as a broad-spectrum bacteriostatic antibiotic, targeting Gram-positive, negative, and anaerobic bacteria. Its mechanism of action focuses on directly blocking the PTC preventing the formation of peptide bonds, and interfering with the binding of tRNA to the A site, effectively inhibiting the protein synthesis [Schlünzen et al., 2001; Oong and Tadi, 2020; National Center for Biotechnology Information, 2025b].

1.4.4 Nitroimidazole

Metronidazole is a compound in the nitroimidazole class, whose mechanism focuses on the production of free nitroso-radicals through its interaction with bacterial nitroreductases. These radicals results cytotoxic in anaerobic bacteria, by damaging the integrity of DNA strands, causing breaks and base modification until cell death, resulting in its definition as bactericidal [Weir and Le, 2019; Edwards, 1993].

Problem statement 2

The human gut microbiota is a complex and diverse community of beneficial bacteria that plays a fundamental role in supporting health. It has various functions, influencing our immune system regulation, digestion, metabolism, defense against harmful pathogens and contributing to the gut-brain axis relation. Disturbance in the diversity or abundance of the gut microbiota, known as dysbiosis, has been linked to various health issues, often with long-lasting consequences.

One of the main causes of dysbiosis is antibiotic usage. These drugs are traditionally categorized as bacteriostatic (inhibiting bacterial growth) or bactericidal (killing bacteria). Depending on their mode of action, antibiotics target both pathogens and commensals in our body, even at low doses from environmental or dietary exposure.

Emerging evidence has shown that certain Protein Synthesis Inhibitors (PSI) antibiotics, classically defined as bacteriostatic, such as macrolides and tetracyclines, manifest bactericidal effects against commensal gut bacteria, contrary to their initial classification [Maier et al., 2021].

The lack of a proper characterization of the effects of antibiotics on our microbiota is caused by using classical model bacteria or common pathogens as system models, in addition to the textbook static-cidal classification of antibiotics. This characterization is still in use in clinics and guides the choice of antibiotic used in treatment. A prior study screened 3 antibiotics and 12 gut bacterial strains and has shown that this classification was not adequate when applied to more diverse microbes such as gut bacterial strains [Maier et al., 2021].

Metagenomic analyses have been extensively used to study the *in vivo* effects of antibiotics on the gut microbiota. Although much data can be obtained through this method, the complexity of the ecology and biochemical pathways, are factors that can influence the analysis resulting in a lack of conclusive studies. To overcome this limit, *in vitro* of individual cultures, and *ex-vivo* communities studies can be parallelly performed to further investigate the impact of antibiotics on bacterial communities.

This research aims to explain whether the bacteriostatic/bactericidal division is maintained when accounting for bacterial diversity, by performing a high-throughput measurement of bacterial survival after antibiotic treatment using 25 relevant and abundant gut bacterial strains with 20 different antibiotics.

This study aims to achieve the following objectives:

- Perform a high-throughput measurement of the Minimum Inhibitory Concentrations (MIC) for 20 antibiotics on 25 gut bacterial strains;
- Develop a method to test the survival of strains of interest in liquid cultures using growth curves;
- Test bacterial survival against the same antibiotics through a classical survival assay with CFU counting;

"Can commonly used antibiotics, both bacteriostatic and bactericidal, exhibit bactericidal effects at clinically relevant concentrations on gut bacteria?"

Experimental Theory 3

3.1 MIC and MBC

The MIC is defined as the lowest concentration that inhibits the visible growth of bacteria in a medium after an overnight incubation. The MIC is a measurement for testing bacteria's sensitivity to a specific antimicrobial substance, such as antibiotics. Methodologically, it is agreed upon a dilution range made through doubling dilution steps starting from 1 mg/L. Along the dilution range, positive control is performed by measuring bacterial growth in the culture medium without the antimicrobial substance. During a 24h incubation, bacterial growth can be measured through optical density (OD) [Andrews, 2001; Wiegand et al., 2008].

The MIC does not evaluate the resistance or provide any insight into the mechanisms or dynamics of the bactericidal/bacteriostatic antibiotics. Depending on the antimicrobial substance used, the inhibition growth might stop once the bacteria is reinoculated in a medium with no antibiotic [Wiegand et al., 2008; Kowalska-Krochmal and Dudek-Wicher, 2021].

The MBC is defined as the lowest concentration of drug in which a subculture of a tested strain will not present any growth in an antibiotic-free media (**figure 3.1**) [Andrews, 2001; Pankey and Sabath, 2004b].

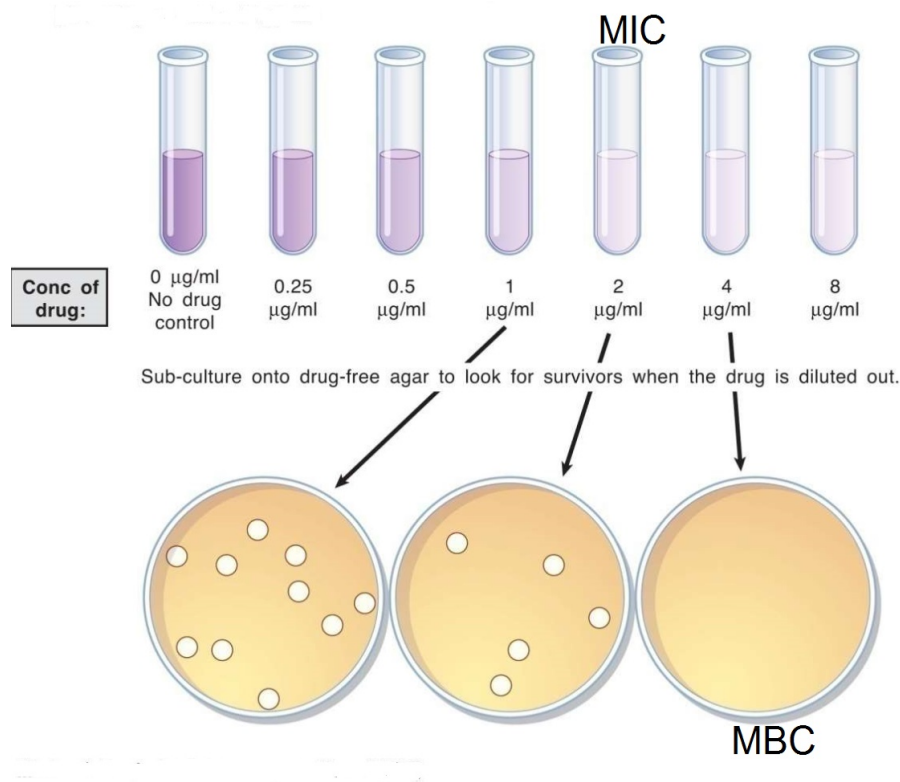


Figure 3.1. Schematics of MIC and MBC techniques performed on a bacterial strain [bio.libretexts.org, 2024]

3.2 Survival assay

Another way to determine antimicrobial activity is through a survival assay [Hossain, 2024]. A survival study determines whether an antibiotic is bactericidal or bacteriostatic. A antibiotic is considered bactericidal when 99.9 % of bacteria die, or alternatively when the number of Colony Forming Units (CFU) is reduced by $\geq 3 - \log_{10}$ CFU/mL. It is considered to be bacteriostatic if a reduction of $< 3 - \log_{10}$ CFU/mL in a time of 5-24h occurs [French, 2006].

A method of interest is the possibility of performing the survival assay at 5x the MIC for antibiotics for a period of 2,4,6 or 24h [Maier et al., 2021; French, 2006].

3.3 Optical Density Measurements

Bacterial growth measurements are one of the most common techniques applied in microbiology, performed by measuring the Optical Density (OD), or absorbance, of a growing bacterial population in a solution at $\lambda = 600\text{nm}$. Through measurements of the OD, we can estimate the concentration, or bacterial number, abiding by the Lambert-Beer law, but only in conditions of lower bacterial densities. Oppositely at higher concentrations, the passing light has multiple unwanted scatterings or interactions with the different bacteria in the media before reaching the detector. Compared to the single scattering in low population cases, the multiple scattering makes the Lambert-beer equation not linear, thus not correlating absorbance to concentration (**Fig. 3.2**). To solve this problem, measurements are kept at lower bacterial concentrations.

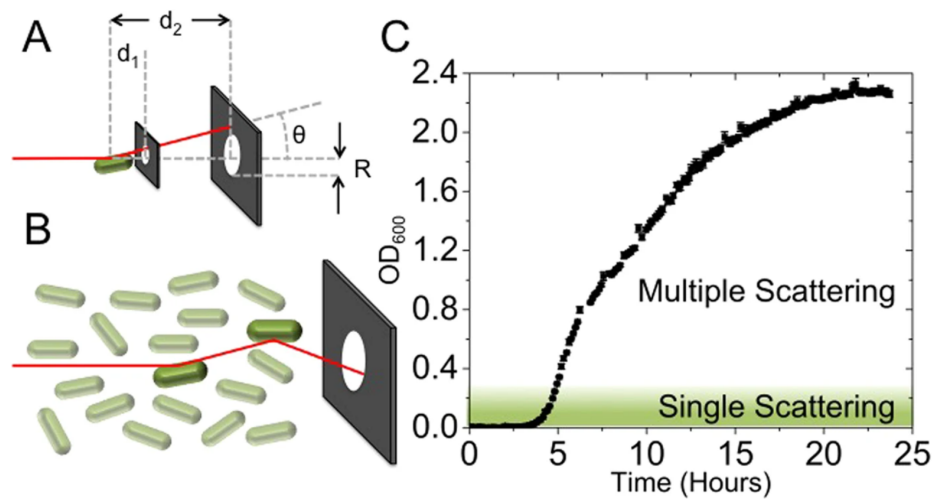


Figure 3.2. (A) Light passing through the bacterial suspension, is scattered at an angle (θ) relative to the optical axis (z). In single scattering, light interacts with only one cell before reaching the detector, but in multiple scattering, light is deflected multiple times as it passes through the sample. The likelihood of scattered light reaching the detector is influenced by its aperture size (R) and the distance between the sample and the detector (d_1 or d_2). (B) As bacterial density increases, multiple scattering becomes more frequent, increasing the chance that scattered light is redirected toward the detector [Stevenson et al., 2016].

Experimental Overview 4

The objective of this study is to first perform an extensive screening to determine the Minimum Inhibitory Concentrations (MIC) of 20 different antibiotics against various strains.

Secondly, through a survival assay, strains of interest are tested by measuring the detection time of growth curves in liquid cultures to determine the CFU/mL as a novel method.

Finally, a more classical survival assay is also performed through spotting on modified Gifu Anaerobic Media (mGAM) agar plates. A decimal dilution for each strain is spotted on agar to determine the [CFU/mL] that there would be without antibiotic, and define it as "t0"; bacteria are treated with antibiotic for 5h and 24h, and then spotted on agar to count the [CFU/mL]. The static-cidal effect of antibiotics is determined by dividing the amount of cells after 24h of treatment, divided by t0.

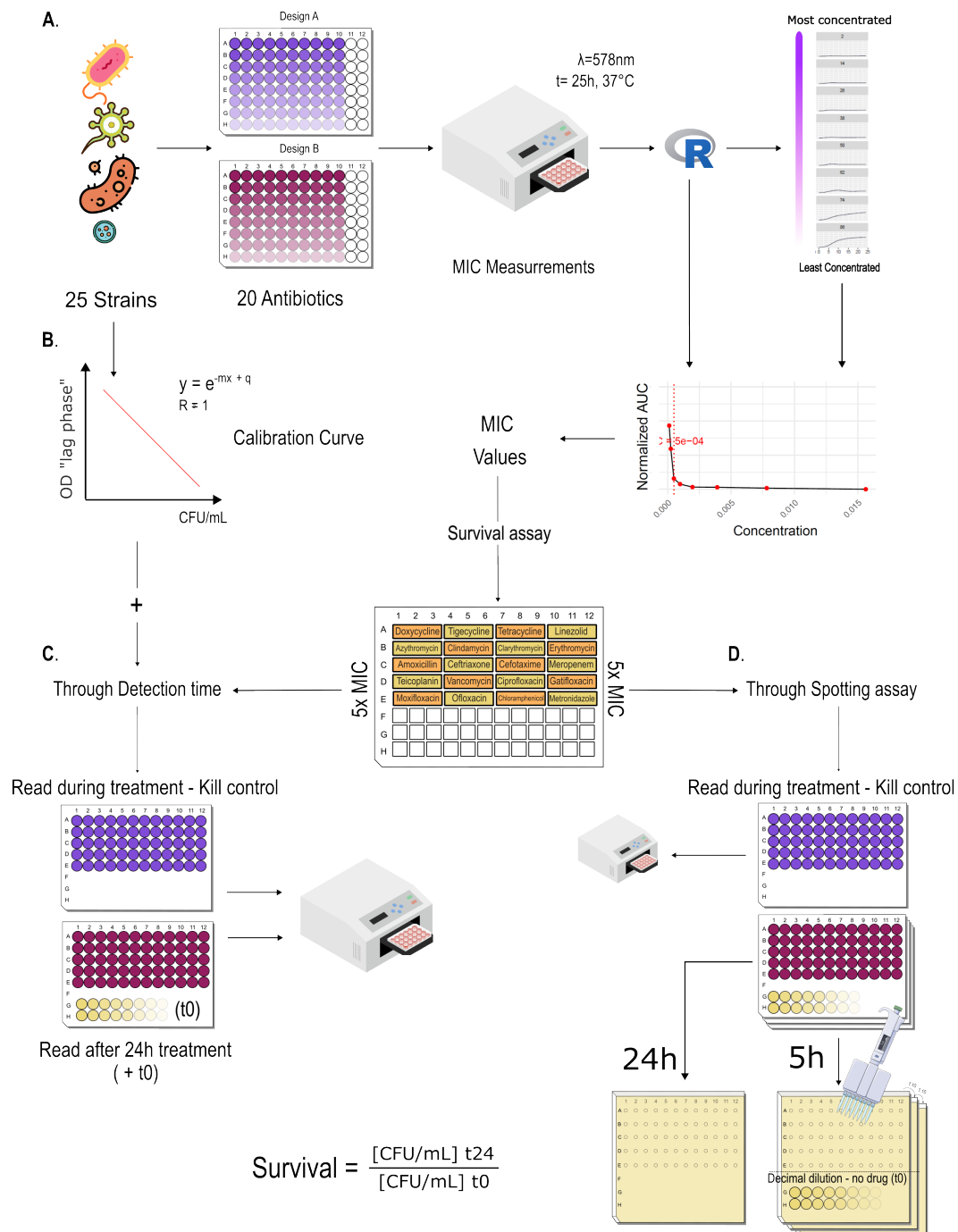


Figure 4.1. Overview of the experimental process. **A.** To study the static-cidal effect of the antibiotics, MIC measurements are needed. Each strain is inoculated in a twofold serial dilution of antibiotics, to determine at which concentration they stop growing (the MIC value). **B.** Calibration curve for each strain are built, this equation puts in correlation the lag time needed to detect bacterial growth, and translates it into a concentration (CFU/mL). **C.** With the calibration curve we can perform a survival assay through detection time (5x MIC) to obtain the number of bacteria present after treatment. A decimal dilution of a strain is made in order to know the number of bacteria without treatment, and, define it as "t0". After a 24h treatment, bacteria will be inoculated in an antibiotic free media, and read to know the amount of bacteria present. A kill control is needed to make sure we are above MIC and bacteria are killed/inhibited. **D.** Static-cidal relation between strain and antibiotic is studied through a survival assay by spotting on agar plates after 5h and 24h of treatment. Survival is calculated by dividing the number of cells left after a 5h or 24h treatment, by the number of cells that there would be in no treatment.

Materials & Methods

5

5.1 Materials and Apparatus

Method	Apparatus	Manufacturer	Model/LOT
Antibiotic Stocks Preparation	Analytical balance	Mettler Toledo	ML104T /00
	96 Deep well plates	Costar	31823000
	96 shallow well plates	Thermo Scientific	182282
	Reservoir	Thermo Scientific	
	Water bath	Grant	JB Aqua 18 (VAB18EU)
MIC Analysis	Anaerobic Chamber	Coy type A	
	Microplate Spectrophotometer	Agilent	EPOCH2NS-SN (23053102)
	96 Deep well plates	Costar	31823000
	96 shallow well plates	Thermo Scientific	182282
	Breathe-Easy Sealing membrane	Merck	MKCW4635
	Deep row reservoirs	Thermo scientific	
CFUs and detection phase counting	Anaerobic Chamber	Coy type A	
	Microplate Spectrophotometer	Agilent	EPOCH2NS-SN (23053102)
	96 Deep well plates	Costar	31823000
	96 shallow well plates	Thermo Scientific	182282
	Breathe-Easy Sealing membrane	Merck	MKCW4635
	Reservoirs	Thermo scientific	
	squared petri dishes	Greiner	F2404359
	96 spotting well plates	Thermo Scientific	182282
Survival Assay	Anaerobic Chamber	Coy type A	
	Microplate Spectrophotometer	Agilent	EPOCH2NS-SN (23053102)
	96 Deep well plates	Costar	31823000
	96 shallow well plates	Thermo Scientific	182282
	Breathe-Easy Sealing membrane	Merck	MKCW4635
	Reservoirs	Thermo scientific	
	Squared petri dishes	Greiner	F2404359
	96 spotting well plates	Thermo Scientific	182282

Table 5.1. Apparatus used in each method.

Method	Compounds	Manufacturer	LOT/Batch
Antibiotic Stocks Preparation	Tigecycline	TCI	
	Teicoplanin	TCI	
	Gatifloxacin	Cayman Chemical	
	Tetracycline	TCI	FHWMF-IQ
	Amoxicillin	Thermo Scientific	
	Cefotaxime	TCI	
	Meropenem	TCI	
	Doxyxycine	TCI	GUP3F-RB
	Linezolid	TCI	E3OGD-ES
	Azithromycin	Cayman Chemical	
	Clindamycin	TCI	IHT5A-AY
	Clarithromycin	TCI	
	Erythromycin	TCI	TCIE0751
	Ceftriaxone	TCI	
	Vancomycin	Combi-block	
	Ciprofloxacin	TCI	
	Moxifloxacin	Combi-block	
	Ofloxacin	TCI	
	Chloramphenicol	TCI	LWUQA-YK
	MilliQ		
	DMSO	Thermo Scientific	Z07J036
	HCl (1N)	Sigma	RNBL6705
	Ethanol	Fisher Chemical	1924448
MIC plates (antibiotics included)	mGAM broth	Shimadzu Diagnostic Co. (AccuDia™)	029312
	Listed Antibiotics		
CFUs and detection phase counting	mGAM broth	Shimadzu Diagnostic Co. (AccuDia™)	029312
	PBS	EPFL	
Survival assay	mGAM broth	Shimadzu Diagnostic Co. (AccuDia™)	029312
	PBS	EPFL	
	Listed Antibiotics		

Table 5.2. Chemicals and compounds used in each method.

Methods 6

6.1 MIC Drug Plates preparation

A set of 20 Antibiotics from different classes of action has been selected, and stocks have been prepared with the following concentrations:

Antibiotic	Solvent	Manufacturer	Concentration
Tigecycline	DMSO	TCI	30 mg/mL
Teicoplanin	Water	TCI	10 mg/mL
Gatifloxacin	Water + ultrasound+ pH 4	Cayman Chemical	0.5 mg/mL
Tetracycline	Ethanol	TCI	10 mg/mL
Amoxicillin	DMSO	Thermo Scientific	10 mg/mL
Cefotaxime	Water	TCI	10 mg/mL
Meropenem	DMSO	TCI	10 mg/mL
Doxycycline	DMSO	TCI	10 mg/mL
Linezolid	DMSO	TCI	10 mg/mL
Azithromycin	DMSO	Cayman Chemical	5 mg/mL
Clindamycin	Water	TCI	10 mg/mL
Clarithromycin	DMSO	TCI	1 mg/mL
Erythromycin	DMSO	TCI	10 mg/mL
Ceftriaxone	PBS - on the day	TCI	10 mg/mL
Vancomycin	Water + heat + pH5	Combi-block	0.5 mg/mL
Ciprofloxacin	Water + heat + pH 3	TCI	0.5 mg/mL
Moxifloxacin	Water + heating	Combi-block	0.5 mg/mL
Ofloxacin	Water + heat + pH 2-5	TCI	2 mg/mL
Chloramphenicol	ethanol	TCI	12.5 mg/mL
Metronidazole	Water+ heating	TCI	10 mg/mL

Table 6.1. List of antibiotics of interest used for the experimental analysis of this study, and their relative stock concentrations

Each antibiotic present in **table 6.1**, was weighed on an analytical balance, dissolved in DMSO, Ethanol, PBS or milliQ water, for a final volume of 10 mL for each solution, and then aliquoted and stored at -24°C. Antibiotics solvated in Milli-Q water were filtered with a 0.22 μm sterile syringe filter.

MIC Plates were prepared in 96-well plates, subdivided into two designs (A and B), **figure 6.2**, containing 10 different antibiotics each. To do this, a 2mL 96-deep well master plate was

prepared with mGAM broth + antibiotic, at different concentrations as stated in the plate designs, and then aliquoted, following the concentration gradient from less to more concentrate to 96-well plates, where bacteria will be later inoculated in the anaerobic chamber. A twofold serial dilution of each antibiotic was applied in the master plate, for final concentrations as seen in **table 6.2** in mGAM Media for each row.

Design A	DOX	TGC	TET	LNZ	AZM	CLI	CLR	ERY	AMX	CRO
Stock [mg/mL]	10	30	10	10	5	10	1	10	10	10
Final 2x Conc.	0,03125	0,0938	0,0313	0,0313	0,0313	0,0313	0,0156	0,0313	0,0313	0,0313
Dilution factor	320	320	320	320	160	320	64	320	320	320
$\mu\text{L}/1.6\text{mL}$ mGAM	5	5	5	5	10	5	25	5	5	5

MIC (A)	DOX	TGC	TET	LNZ	AZM	CLI	CLR	ERY	AMX	CRO
A [mg/mL]	0,0156	0,0469	0,0156	0,0156	0,0156	0,0156	0,0078	0,0156	0,0156	0,0156
B [mg/mL]	0,0078	0,0234	0,0078	0,0078	0,0078	0,0078	0,0039	0,0078	0,0078	0,0078
C [mg/mL]	0,0039	0,0117	0,0039	0,0039	0,0039	0,0039	0,0020	0,0039	0,0039	0,0039
D [mg/mL]	0,0020	0,0059	0,0020	0,0020	0,0020	0,0020	0,0010	0,0020	0,0020	0,0020
E [mg/mL]	0,0010	0,0029	0,0010	0,0010	0,0010	0,0010	0,0010	0,0010	0,0010	0,0010
F [mg/mL]	0,0005	0,0015	0,0005	0,0005	0,0005	0,0005	0,0002	0,0005	0,0005	0,0005
G [mg/mL]	0,0002	0,0007	0,0002	0,0002	0,0002	0,0002	0,0001	0,0002	0,0002	0,0002
H [mg/mL]	0,0001	0,0004	0,0001	0,0001	0,0001	0,0001	0,0001	0,0001	0,0001	0,0001

Design B	CTX	MEM	TEC	VAN	CIP	GAT	MXF	OFX	CHL	MTZ
Stock [mg/mL]	10	10	10	0,5	0,5	0,5	0,5	2	12,5	10
Final 2x Conc.	0,03125	0,0313	0,0313	0,0313	0,0313	0,0313	0,0156	0,0313	0,0313	0,0313
Dilution factor	320	320	320	16	16	16	32	64	400	320
$\mu\text{L}/1.6\text{mL}$ mGAM	5	5	5	100	100	100	50	25	4	5

MIC (B)	CTX	MEM	TEC	VAN	CIP	GAT	MXF	OFX	CHL	MTZ
A [mg/mL]	0,0156	0,0156	0,0156	0,0156	0,0156	0,0156	0,0078	0,0156	0,0156	0,0156
B [mg/mL]	0,0078	0,0078	0,0078	0,0078	0,0078	0,0078	0,0039	0,0078	0,0078	0,0078
C [mg/mL]	0,0039	0,0039	0,0039	0,0039	0,0039	0,0039	0,0020	0,0039	0,0039	0,0039
D [mg/mL]	0,0020	0,0020	0,0020	0,0020	0,0020	0,0020	0,0010	0,0020	0,0020	0,0020
E [mg/mL]	0,0010	0,0010	0,0010	0,0010	0,0010	0,0010	0,0005	0,0010	0,0010	0,0010
F [mg/mL]	0,0005	0,0005	0,0005	0,0005	0,0005	0,0005	0,0002	0,0005	0,0005	0,0005
G [mg/mL]	0,0002	0,0002	0,0002	0,0002	0,0002	0,0002	0,0001	0,0002	0,0002	0,0002
H [mg/mL]	0,0001	0,0001	0,0001	0,0001	0,0001	0,0001	0,0001	0,0001	0,0001	0,0001

Table 6.2. In "Design A", the antibiotics Doxycycline: DOX, Tigecycline: TGC, Tetracycline: TET, Linezolid: LNZ, Azithromycin: AZM, Clindamycin: CLI, Clarithromycin: CLR, Erythromycin: ERY, Amoxicillin: AMX, Ceftriaxone: CRO, have been used, with two rows dedicated to positive controls (no antibiotics). For "Design B", the antibiotics Cefotaxime: CTX, Meropenem: MEM, Teicoplanin: TEC, Vancomycin: VAN, Ciprofloxacin: CIP, Gatifloxacin: GAT, Moxifloxacin: MXF, Ofloxacin: OFX, Chloramphenicol: CHL, Metronidazole: MTZ. Each design for each strain has been run in duplicates.

A total of 40 strains of interest are to be analysed as listed in **table 6.3**

Internal ID	Species	NCBI tax ID
NT5001	<i>Phocaeicola vulgatus</i>	435590
NT5002	<i>Bacteroides uniformis</i>	411479
NT5003	<i>Bacteroides fragilis</i> (NT)	272559
NT5004	<i>Bacteroides thetaiotaomicron</i>	226186
NT5006	<i>Clostridium ramosum</i>	445974
NT5009	<i>Eubacterium rectale</i>	657318
NT5011	<i>Roseburia intestinalis</i>	536231
NT5017	<i>Veillonella parvula</i>	479436
NT5019	<i>Prevotella copri</i>	537011
NT5021	<i>Akkermansia muciniphila</i>	349741
NT5022	<i>Bifidobacterium adolescentis</i>	367928
NT5024	<i>Eggerthella lenta</i>	479437
NT5025	<i>Fusobacterium nucleatum</i>	190304
NT5026	<i>Clostridium bolteae</i>	411902
NT5028	<i>Bifidobacterium longum</i>	565042
NT5032	<i>Clostridium perfringens</i>	451754
NT5033	<i>Bacteroides fragilis</i> (ET)	272559
NT5036	<i>Bilophila wadsworthia</i>	1408428
NT5037	<i>Clostridium saccharolyticum</i>	610130
NT5038	<i>Streptococcus salivarius</i>	1420586
NT5042	<i>Lactocaseibacillus paracasei</i>	321967
NT5045	<i>Ruminococcus bromii</i>	Not in library
NT5046	<i>Ruminococcus gnavus</i>	411470
NT5047	<i>Ruminococcus torques</i>	411460
NT5048	<i>Clostridium comes</i>	470146
NT5050	<i>Bacteroides caccae</i>	411901
NT5054	<i>Bacteroides ovatus</i>	411476
NT5064	<i>Bacteroides rylanisolvans</i>	997892
NT5069	<i>Blautia obeum</i>	411459
NT5071	<i>Parabacteroides merdae</i>	411477
NT5072	<i>Streptococcus parasanguinis</i>	760570
NT5073	<i>Clostridium aerofaciens</i>	411903
NT5074	<i>Parabacteroides distasonis</i>	435591
NT5075	<i>Eubacterium eligens</i>	515620
NT5076	<i>Dorea formicigenerans</i>	411461
NT5077	<i>Escherichia coli</i> IAI1	585034
NT5078	<i>Escherichia coli</i> ED1a	585397
NT5079	<i>Roseburia hominis</i>	585394
NT5081	<i>Oscillibacter splanchnicus</i>	709991
NT5083	<i>Clostridioides difficile</i>	1496

Table 6.3. Selected strains based on the most common present biodiversity in the human gut microbiota Maier et al. [2018]. *B. fragilis* NT stands for "Nontoxigenic", while *B. fragilis* ET stands "Enterotoxigenic"

6.2 MIC analysis

In an anaerobic chamber (Gas mixture: 5% H₂, 12% CO₂, and N₂), strains of interest have been streaked out from glycerol stocks on mGAM agar media, previously left to acclimate overnight in anaerobic condition to remove remaining oxygen, and left to incubate overnight at 37°C. Thereafter, 5mL mGAM broth has been aliquoted in tubes; single colonies of the strains have been inoculated in the broth and incubated overnight at 37°C inside the anaerobic chamber. In an 8-row reservoir, 25 mL of mGAM were aliquoted per row, inoculating 250 μ L of the previously broth-grown overnight cultures, keeping a dilution of 1:100. Thereafter, bacteria cultures have been distributed with 450 μ L aliquots per well in 4 rows of a 2mL 96-deep well plate that will be defined as "master plate".

Each row of the previously described master plate was dedicated to one MIC plate to ensure no cross-contamination. MIC plates from designs A and B (and their duplicates) have been inoculated each with 50 μ L. Inoculation is performed by taking into consideration the gradient of dilution of the antibiotics. MIC plates are then sealed with a gas permeable membrane seal, analysed with a microplate reader at OD578 for 24h at 37°C (**figure 6.1**).

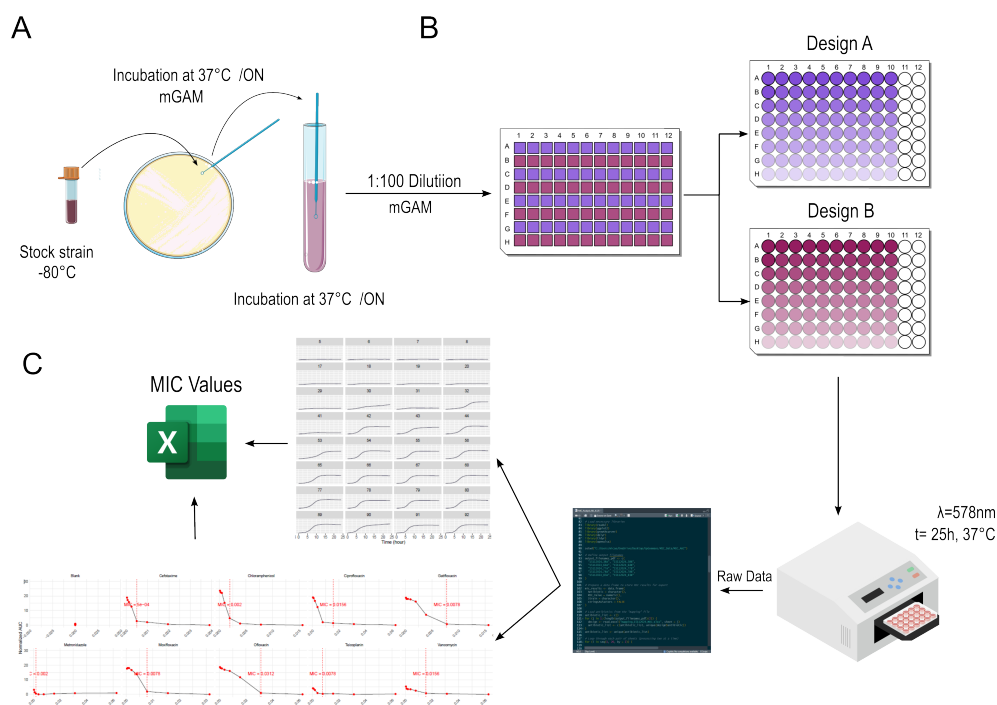


Figure 6.1. Overview of the MIC Protocol. **A**, selection of the strain of interest from the glycerol stock to the liquid media of a single colony. **B**, After a 1:100 dilution of our OverNight (ON) grown culture, strains are inoculated onto the different design plates with antibiotics previously prepared. **C**, Data analysis from Raw Data given by the plate reader, to the actual MIC Values through an R SCRIPT for their detection and graph elaboration [R Core Team, 2021]. A wavelength of $\lambda=578$ nm, is used due to the rich mGAM media.

An example of design is seen in **table 6.2**; after a first look at the phenotypic response to the various antibiotics used, the concentration range is adapted depending on the sensitivity of bacteria to the antibiotic and the test is repeated if necessary, to obtain the MIC.

6.2.1 Script for MIC breakpoint detection

Data from the MIC screening were analysed and extracted using an R Script [R Core Team, 2021]. To find the MIC, raw data is processed first to display growth curves at various concentrations per column. The growth curve graphs are subsequently plotted using the package "growthcurver", to calculate the normalised Area Under Curve (AUC) and as the y-axis of the plot, against the concentration on the x-axis [Sprouffske, 2020].

The script follows a series of conditions to determine the MIC breakpoint, or the concentration at which bacteria do not grow. To determine the MIC, the first and last 3 AUC values from each a line were considered: the closest value to the intersection of these lines is noted as the MIC. To ensure a more accurate selection, a threshold of >98% to find the effective breakpoint. The MIC values are then returned in an Excel file with concentrations in mg/mL, and returning NA for no growth.

6.3 Colony Forming Units and detection time counting

Building the calibration curve, requires parallel spotting of decimal dilution, to determine the [CFU/mL] concentration for each strain, and the reading to these dilutions to obtain the detection time. We define as detection time, the time needed for the detector to read the "lag phase" at each dilution. For each detection time value, there will be a corresponding [CFU/mL] value, obtaining a graph and its equation as shown in **figure 6.2**. All material and media are to be left inside the anaerobic chamber overnight to remove any oxygen and maintain an anaerobic environment.

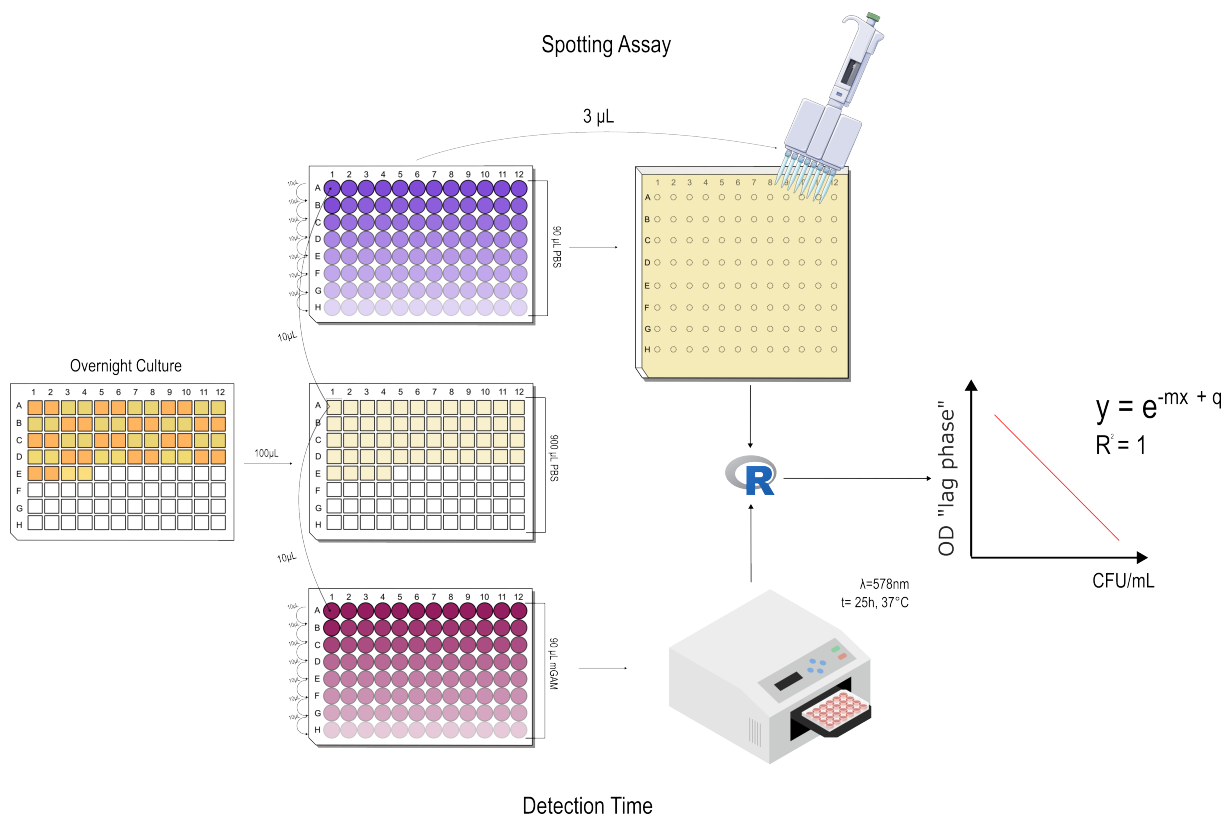


Figure 6.2. Workflow of the building of a calibration curve. This will be performed for each strain of interest, resulting in an exponential equation relating the difference in "lag phase" or detection time, and the cell concentration per mL

6.3.1 Spotting assay

In a 96-well spotting plate, 90 μL of PBS 1x were aliquoted, covered with a breathable seal, and introduced into the anaerobic chamber. In anaerobic conditions, in a 2mL 96-deep well plate, single colonies from the streaked bacteria were inoculated with a pipette tip in each well in 1mL mGAM media and left to grow overnight at 37°C.

The overnight cultures were then mixed by pipetting up and down, and 100 μL were aliquoted in a new deep well plate with 900 μL of PBS 1x, to ensure a dilution of 1:10. Thereafter, 10 μL were then aliquoted in the previously prepared 96 well spotting plates and a serial decimal dilution was performed in the plate, by taking 10 μL from the starting row. In squared mGAM agar plates, 3 μL of each serial dilution per strain were spotted and left to dry, then incubated at 37°C overnight.

6.3.2 Detection time

In 96-well plates, 90 μL of mGAM were aliquoted, skipping the first row, covered with a breathable seal, and introduced into the anaerobic chamber. In anaerobic conditions, in a 96-deep well plate, single colonies from the streaked bacteria were inoculated with a pipette tip in each well in 1mL mGAM media, sealed, and left to grow overnight at 37°C.

The overnight cultures were then mixed by pipetting up and down, and 100 μL were aliquoted in a new deep well plate with 900 μL of PBS 1x, to ensure a dilution of 1:100. Hereafter, 10 μL were then aliquoted in the previously prepared 96 well plates and a serial decimal dilution was performed in the plate, by taking 10 μL from the starting row. Replicates of each plate were read on the plate reader at $\lambda=578$, for 24h at 37°C.

6.4 Survival Assay through detection time count

Once the MIC values and the calibration curve are obtained, a survival assay can be performed.

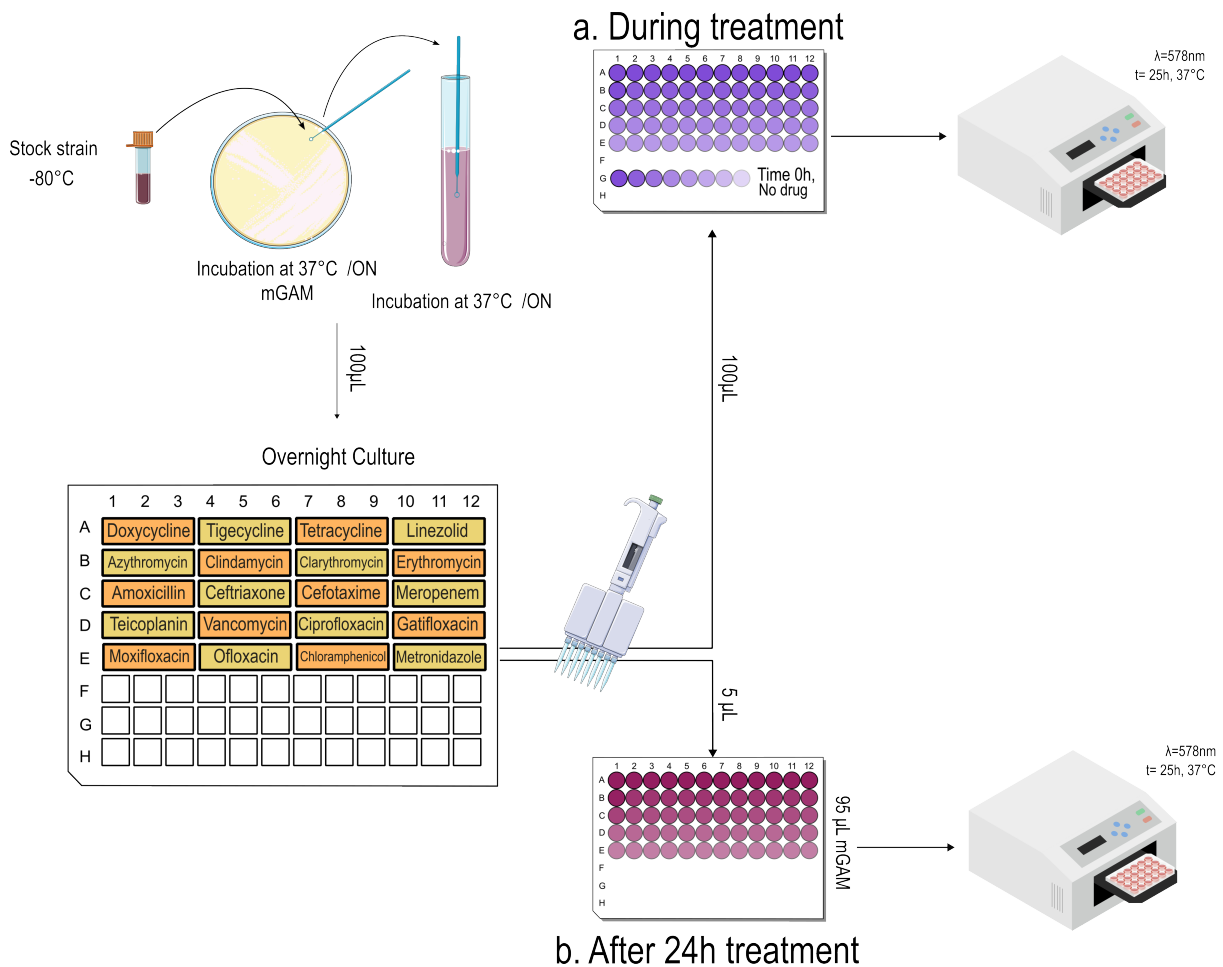


Figure 6.3. Workflow of survival assay in liquid through detection time, or the amount of time needed to detect a high enough cell count to see the start of the log phase. This value can be converted that in a concentration thanks to the calibration curve. **a.** In the first plate, a kill control is performed to confirm that we are indeed at 5x above MIC and check if there is no growth. **b.** After a 24h treatment, we inoculate cells in a new media without antibiotic and read once again to see when the growth starts and determine the detection time

In a 0.5mL 96-deep well plate, the 20 antibiotics of interest are aliquoted to result in a final concentration 10 times the MIC specific to each strain, in 100 µL of mGAM. 3 replicates were conducted for each antibiotic. In the same plate, one row will be dedicated for a serial decimal dilution to detect growth at time 0, where all wells are filled with 90 µL mGAM except for the first one. This is performed for each strain as illustrated in **table 6.4**. The plate is left overnight in the anaerobic chamber covered with aluminium foil to avoid photodegradation of the antibiotics.

In parallel, overnight cultures are prepared in a 96-deep well plate, single colonies from the streaked bacteria are inoculated with a pipette tip in each well in 1mL mGAM media, sealed, and left to grow overnight at 37°C.

The following day, in an 8-deep row reservoir, 20 μ L of the overnight-grown strains are inoculated in 10 mL of mGAM per row, and 200 μ L for the slow-growing strains: NT5006, NT5019, NT5024, and NT5037. Hereafter, 100 μ L are aliquoted per well in the antibiotic plate and mixed by pipetting up and down. With the same tips, 100 μ L are transferred in an OD 96-well plate, sealed, and placed in the plate reader to read at OD578, at 37°C for 24h.

Antibiotic plates containing the strains are then incubated at 37°C for 24h. The following day, in a new OD 96-well plate previously prepared with 95 μ L mGAM, 5 μ L from the drug plate are inoculated, and placed to read in the same conditions.

		1	2	3	4	5	6	7	8	9	10	11	12
10x MIC mg/mL	A	DOX			TIG			TET			LNZ		
	B	AZM			CLI			CLR			ERY		
	C	AMX			CRO			CTX			MEM		
	D	TEC			VAN			CIP			GAT		
	E	MXF			OFX			CHL			MTZ		
	F												
	G		CALIBRATION CURVE										
	H												

Table 6.4. Design plate for survival-Assay for each strain. If a strain was deemed as resistant, or with an MIC breakpoint $> 0.031\text{mg/mL}$, the assay was not performed, given the high concentration for most clinical breakpoints. Doxycycline: DOX, Tigecycline: TGC, Tetracycline: TET, Linezolid: LNZ, Azithromycin: AZM, Clindamycin: CLI, Clarithromycin: CLR, Erythromycin: ERY, Amoxicillin: AMX, Ceftriaxone: CRO, Cefotaxime: CTX, Meropenem: MEM, Teicoplanin: TEC, Vancomycin: VAN, Ciprofloxacin: CIP, Gatifloxacin: GAT, Moxifloxacin: MXF, Ofloxacin: OFX, Chloramphenicol: CHL, Metronidazole: MTZ.

6.5 Survival Assay through spotting assay

A more classical survival assay was performed with measuring of static-cidal activity, by spotting at time-point 5h and 24h of treatment.

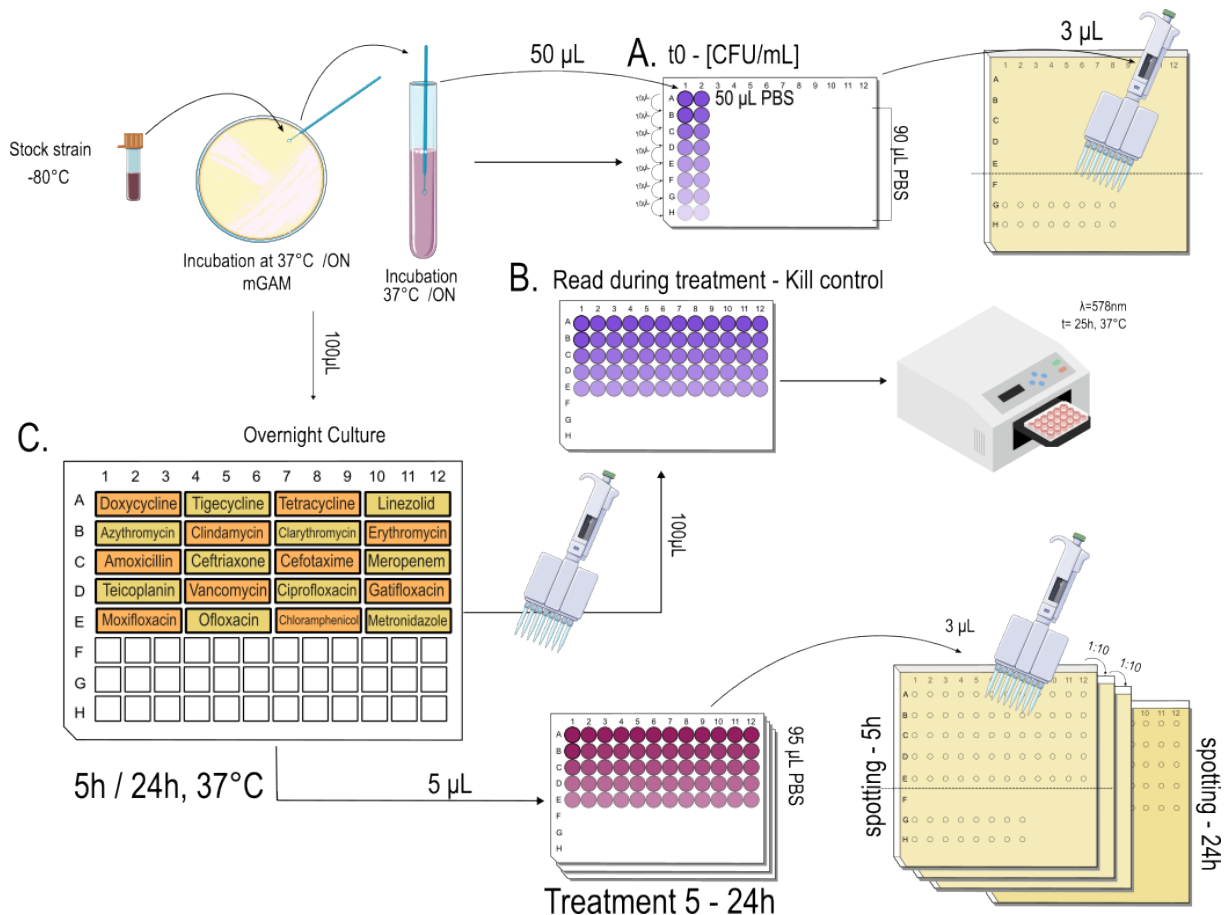


Figure 6.4. Workflow of survival assay, with spotting. **A.** To obtain the [CFU/mL] at "t0", without antibiotic treatment, a decimal serial dilution is spotted on mGAM agar and the counted. **B.** Bacteria are inoculated from the overnight culture to the drug plate: 100 µL are read during treatment to ensure no growth and the antibiotic concentration is over the MIC. **C.** After a treatment 5h a decimal dilution is performed 3 times and each spotted to ensure a countable amount of CFUs. After 24h of treatment 3 µL are spotted once again. With the [CFU/mL] of t24h and t0, we can calculate the static-cidal activity of antibiotics.

A 0.5mL deep well plate with the antibiotic of interest was prepared as shown in **table 6.4** with antibiotic concentration at 10x the MIC for each specific strain, for a final volume of 100µL. The prepared plate and mGAM agar squared plates were left to rest overnight in the anaerobic chamber to remove oxygen; overnight cultures of the strains were prepared in mGAM broth and left to grow overnight. Hereafter, 20 µL of the overnight culture was aliquoted into 10 mL mGAM and pregrown for 1-2h at 37°C (dilution 1:500).

To obtain time 0h, in a shallow 96-well plate, 50 μL of PBS were aliquoted in each well of the first row only, for as many strains as analysed, where 50 μL will be inoculated in (1:1000 dilution). In the rest of the wells, 90 μL of PBS were aliquoted, and a serial decimal dilution was performed (10 μL from one well to the following one), with tips changed at every dilution.

Hereafter, 3 μL were spotted with a multichannel pipette on the mGAM square plate, and allowed to dry; plates were incubated for 48h at 37°C. In parallel, on the prepared drug plate, 100 μL of pregrown overnight culture was added to each well with a multichannel pipette, mixed by pipetting up and down, and tips were changed every time. For each well, 100 μL was aliquoted into an OD 96-well plate to be read for 24h at 37°C, and the drug plate was left to incubate for a timepoint at 5h and 24h. For each time point, in a shallow 96-well plate, 5 μL was aliquoted into 95 μL of PBS (1:20 dilution), and 3 μL was spotted on a squared mGAM plate. Decimal dilutions are performed 3 times and spotted: mGAM plates are left to dry, and then incubated for 48h at 37°C.

6.6 Phylogenic tree

To create the phylogenic tree of the strains used in this study, ribosomal 16s sequences were downloaded from the NCBI Database [Sayers et al., 2022]. Due to the high similarity and conservation of the 16s rRNA, strains of the same species might have the same sequence analysed. With the use of "BioEdit Sequence Alignment Editor software" [Hall et al., 1999]; Aminoacidic sequences were aligned through ClustalW Multiple Alignment (Full multiple alignment, Bootstrap NJ tree, with 1000 bootstraps) [Thompson et al., 1994]. An edit was performed on the aligned sequences by trimming the excess ends of sequences of strains NT5050, NT5054, NT5064, NT5077, and NT5083.

Trimming of the sequence ends was done to remove poorly aligned longer sequences and diminish noise that might come with them while building the tree. However, recent studies suggest that the editing of these extremities might lead to more inaccurate results [Portik and Wiens, 2020]. In the case of 16s ribosomal RNA sequences, trimming is not thought to be a problem, due to their highly conserved nature. To support this, both trees have been run with the same parameters, except for the trimming: the resulting output did not present any change. Thereafter, the aligned data is analysed and run through MEGA11 software to create the tree using maximum likelihood as a statistical method, with the following parameters: a test of phylogeny – Bootstrap method (100 n° of replication), TN93+G+I model – n° of discrete gamma categories (4).

7.1 MIC Measurement

MICs for commensal strains were measured to characterise the sensitivity of the bacterial strains to the compounds of interest (**table 6.1**). Of the 40 selected gut microbiota strains, hard-to-grow species on mGAM were removed, obtaining a final total of 25 strains, listed in (**table 7.1**), whose sensitivity was tested against 20 antibiotics of interest.

Species	Strain
<i>P. vulgatus</i>	NT5001
<i>B. uniformis</i>	NT5002
<i>B. fragilis nontoxigenic (NT)</i>	NT5003
<i>B. thetaiotaomicron</i>	NT5004
<i>C. ramosum</i>	NT5006
<i>P. copri</i>	NT5019
<i>B. adolescentis</i>	NT5022
<i>E. lenta</i>	NT5024
<i>C. bolteae</i>	NT5026
<i>C. perfringens</i>	NT5032
<i>B. fragilis enterotoxigenic (ET)</i>	NT5033
<i>C. saccharolyticum</i>	NT5037
<i>S. salivarius</i>	NT5038
<i>R. gnavus</i>	NT5046
<i>C. comes</i>	NT5048
<i>P. merdae</i>	NT5071
<i>S. parasanguinis</i>	NT5072
<i>C. aerofaciens</i>	NT5073
<i>P. distasonis</i>	NT5074
<i>B. caccae</i>	NT5050
<i>B. ovatus</i>	NT5054
<i>B. xylanisolvens</i>	NT5064
<i>E. coli IAI1</i>	NT5077
<i>C. difficile</i>	NT5083
<i>E. coli ED1a</i>	NT5078

Table 7.1. Selected anaerobic strains for MIC measurement and survival assay

In this study, bacteria that have an MIC of > 0.031 mg/mL were considered resistant. The heatmap shown in (**figure 7.2**) gives us a clear overview of the sensitivity of each bacterial strain to each tested antibiotic. Raw data obtained from the plate reader were analysed with a tailor-made script outputting growth curves for each dilution and transformed to obtain a single graph analyzing the area under the curve of each growth curve, and plotting it as a number over a concentration range, as shown in **figure 7.1**). All resulting analysed data was then clustered, where each tile in (**figure 7.2**) is the MIC that indicates the minimum concentration at which the growth of the bacteria is inhibited.

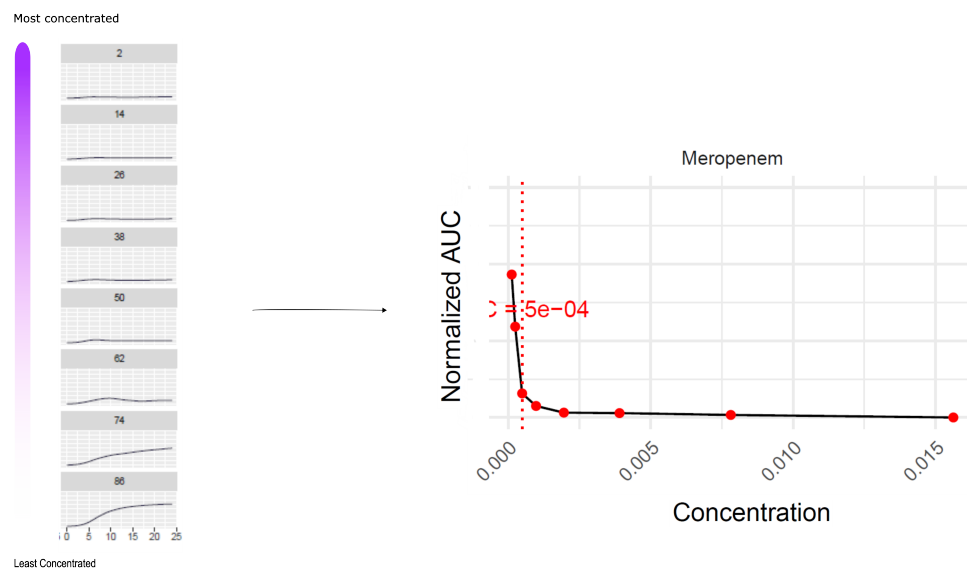


Figure 7.1. Raw data is converted into a series of growth curves, each plot is the growth curve of bacteria + antibiotic present in one well. A series of dilutions shows the inhibition of the growth of the bacteria, which can be measured by taking into consideration the Area Under the Curve (AUC). The R script determines the lowest point before there is no growth, determining it as the MIC

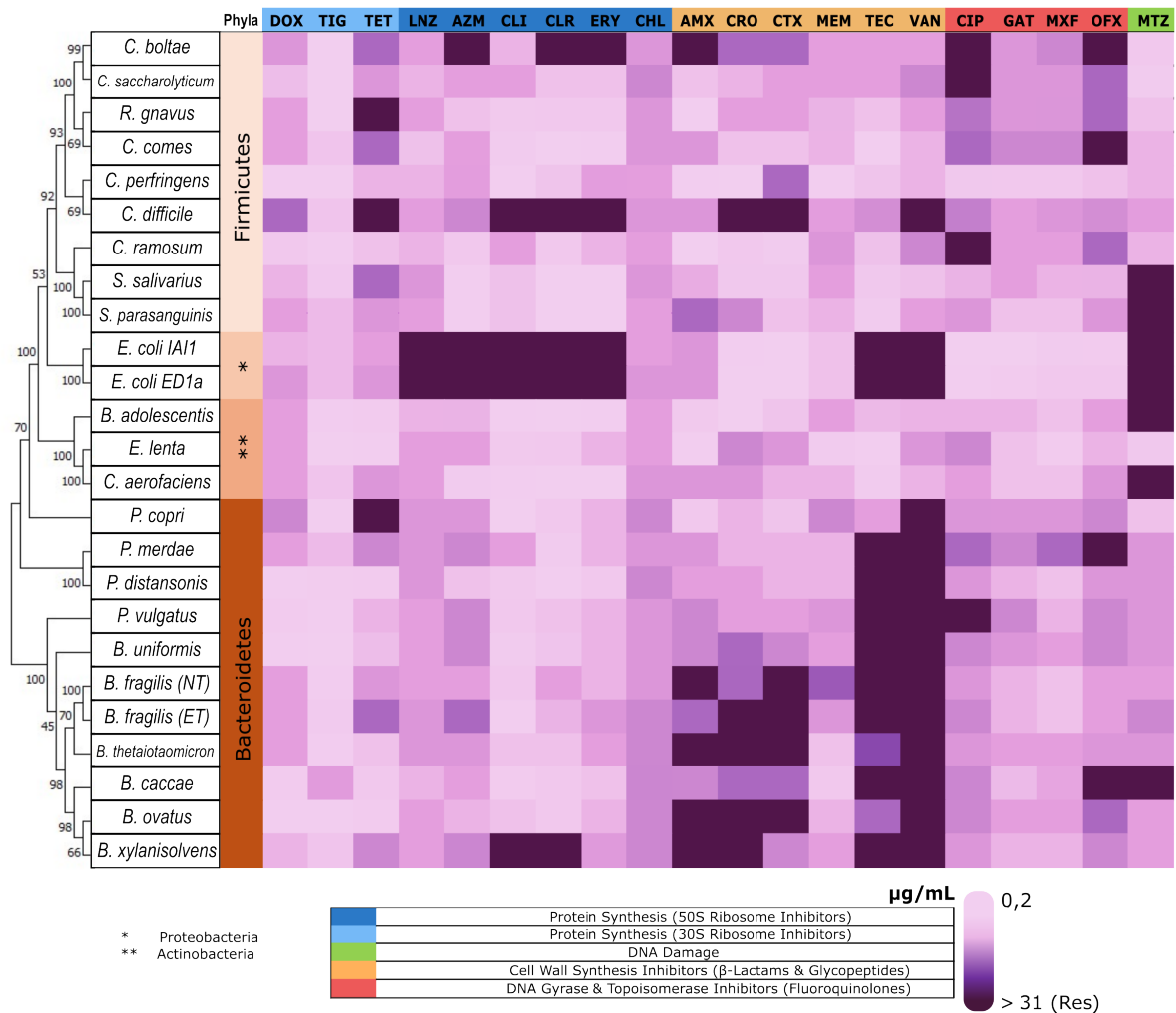


Figure 7.2. Heatmap of bacteria sensitivity to antibiotics. Strains of interest have been rearranged to compare sensitivity to antibiotics based on their phylogeny (Phylogenetic Tree: 100 bootstraps - TN93+G+I). Light purple indicates sensitivity to the antibiotic, whilst darker purple represents gradually more resistance. The tested antibiotic range goes from 0 to 0.625 mg/mL of antibiotic.

7.2 CFU concentration to detection time relationship

Calibration curves relate the detection time, defined as the time needed for bacteria to multiply enough to be detectable, more improperly the "lag phase", and the number of CFUs per millilitre (figure 7.3).

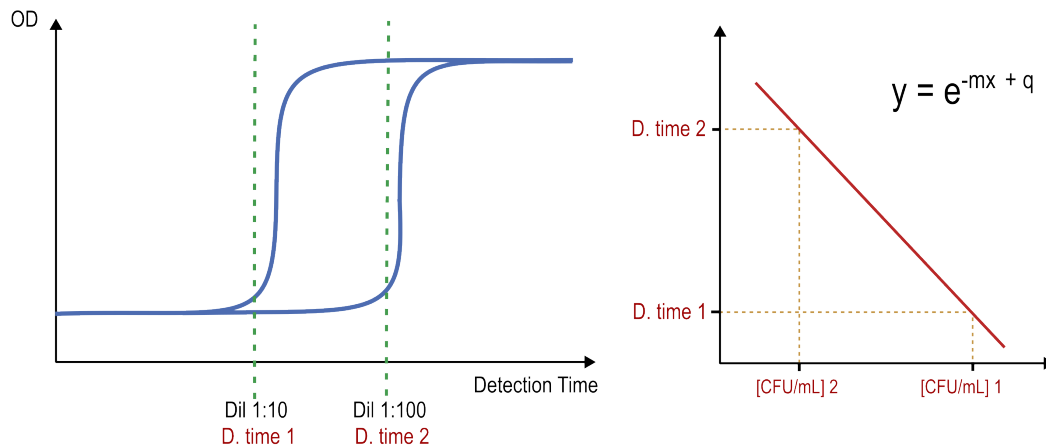


Figure 7.3. At different concentrations, the lag time needed for the bacterial count to be detectable varies. It is therefore possible to correlate lag time to CFU/mL.

Calibration curves are built to measure CFUs in high-throughput measurements in a survival assay through detection time, without the need for spotting on agar plates, therefore improving the efficiency of the screening by saving time, material, and space, allowing more samples to be run at the same time. Equations for each strain are generated, and the following data is obtained, as listed in **table 7.2**. All operations were performed under anaerobic conditions.

Species	Strain	Slope	Intercept	R ²
<i>C. comes</i>	NT5048	-1,2043	10,68	0,99
<i>R. gnavus</i>	NT5046	-1,0034	11,68	0,98
<i>C. bolteae</i>	NT5026	-0,9031	12,83	0,99
<i>C. saccharolyticum</i>	NT5037	-0,7395	15,66	0,99
<i>C. perfringens</i>	NT5032	-2,0792	11,88	0,82
<i>C. difficile</i>	NT5083	-1,4445	19,96	0,95
<i>C. ramosum</i>	NT5006	-1,7517	14,85	0,97
<i>S. salivarius</i>	NT5038	-0,9285	6,00	0,85
<i>S. parasanguinis</i>	NT5072	-1,7834	13,53	0,93
<i>E. coli</i> IAI1	NT5077	-2,0479	11,50	0,9
<i>E. coli</i> ED1a	NT5078	-1,4378	20,97	0,95
<i>B. adolescentis</i>	NT5022	-0,6907	10,66	0,98
<i>E. lenta</i>	NT5024	-1,0510	15,11	0,85
<i>C. aerofaciens</i>	NT5073	-0,8895	13,95	0,99
<i>P. copri</i>	NT5019	-6,7054	1,71	0,91
<i>P. merdae</i>	NT5071	-0,5745	9,57	1
<i>P. distasonis</i>	NT5074	-0,5676	12,96	0,99
<i>P. vulgatus</i>	NT5001	-0,9574	14,89	0,99
<i>B. uniformis</i>	NT5002	-0,7668	14,73	0,97
<i>B. fragilis nontoxigenic (NT)</i>	NT5003	-1,0231	16,11	0,98
<i>B. fragilis enterotoxigenic (ET)</i>	NT5033	-0,8460	13,85	0,99
<i>B. thetaiotaomicron</i>	NT5004	-0,9215	15,84	0,88
<i>B. caccae</i>	NT5050	-1,0233	14,56	0,99
<i>B. ovatus</i>	NT5054	-0,9321	12,99	0,95
<i>B. xylanisolvens</i>	NT5064	-0,8968	13,59	0,97

Table 7.2. Slope and Intercept from the exponential equation of the calibration curve with their respective R². All calibration curves can be found in **appendix 11.1**

7.3 Survival Assay through detection time counting

The objective of this assay is to measure the survival of the strains after the antibiotic treatment, by measuring the time needed to detect cell growth, comparing the detection time at time 0h and at time 24h.



Figure 7.4. **A.** Read of bacteria growth during antibiotic treatment, **B.** Read of Bacteria in order to qualitatively see regrowth. (*B. caccae*), NT5050.

Few fast-growing strains show more plausible results as shown in **figures (7.4)**, and **(7.5)** as an example, compared to other strains; Depending on the strain, the static-cidal activity of each antibiotic is different. For example, in **figures (7.4)**, and **(7.5)**, the growth of strain NT5074 is inhibited in the presence of doxycycline, but not when re-inoculated in fresh medium without doxycycline. This classifies doxycycline as a bacteriostatic antibiotic for NT5074.

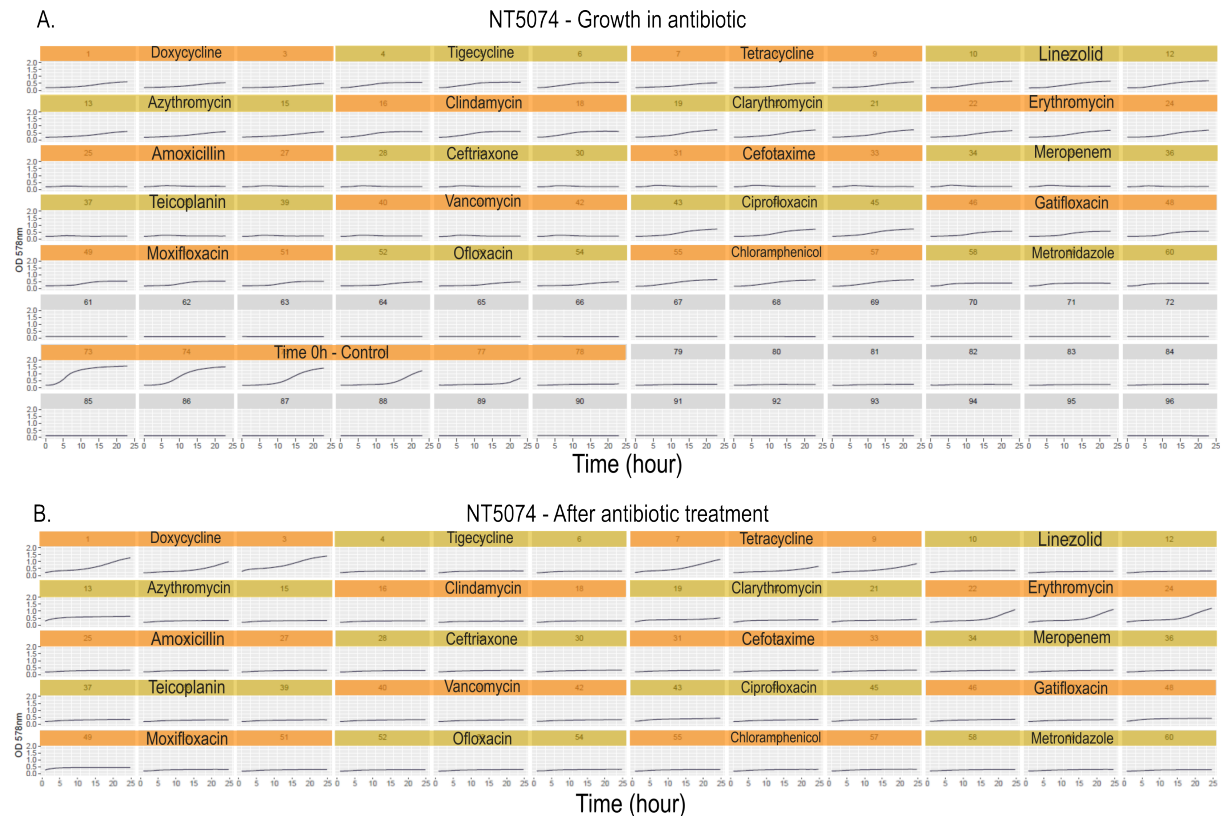


Figure 7.5. **A.** Growth in antibiotics is used to also determine if concentrations are indeed above the MIC and inhibiting bacterial growth; **B.** Bacterial growth present in the first plate and not in the second can be attributed to dead cells being detected by the reader, justified by no growth on the second plate (*P. distasonis*), NT5074.

Strain NT5002, *B. uniformis* was used as an example to test the methodology further. No detection time is seen across the plate as seen in **figure 7.6-A**, except for Erythromycin, showing a start of growth towards the 23rd hour.

Suspecting a low detection time due to a low number of starting cells, the experiment was thus repeated, reading growth at a total of 48h, which allowed for growth, as seen in **figure 7.6-B**. To test this low count hypothesis, strain NT5002 was treated as usual with antibiotic for 24h and then spotted directly on mGAM agar undiluted, and then compared to a spotting after a 1:20 dilution of the treated bacterial cells. The undiluted spotting shows more probable results, showing growth also in linezolid, as expected, compared to the undiluted.

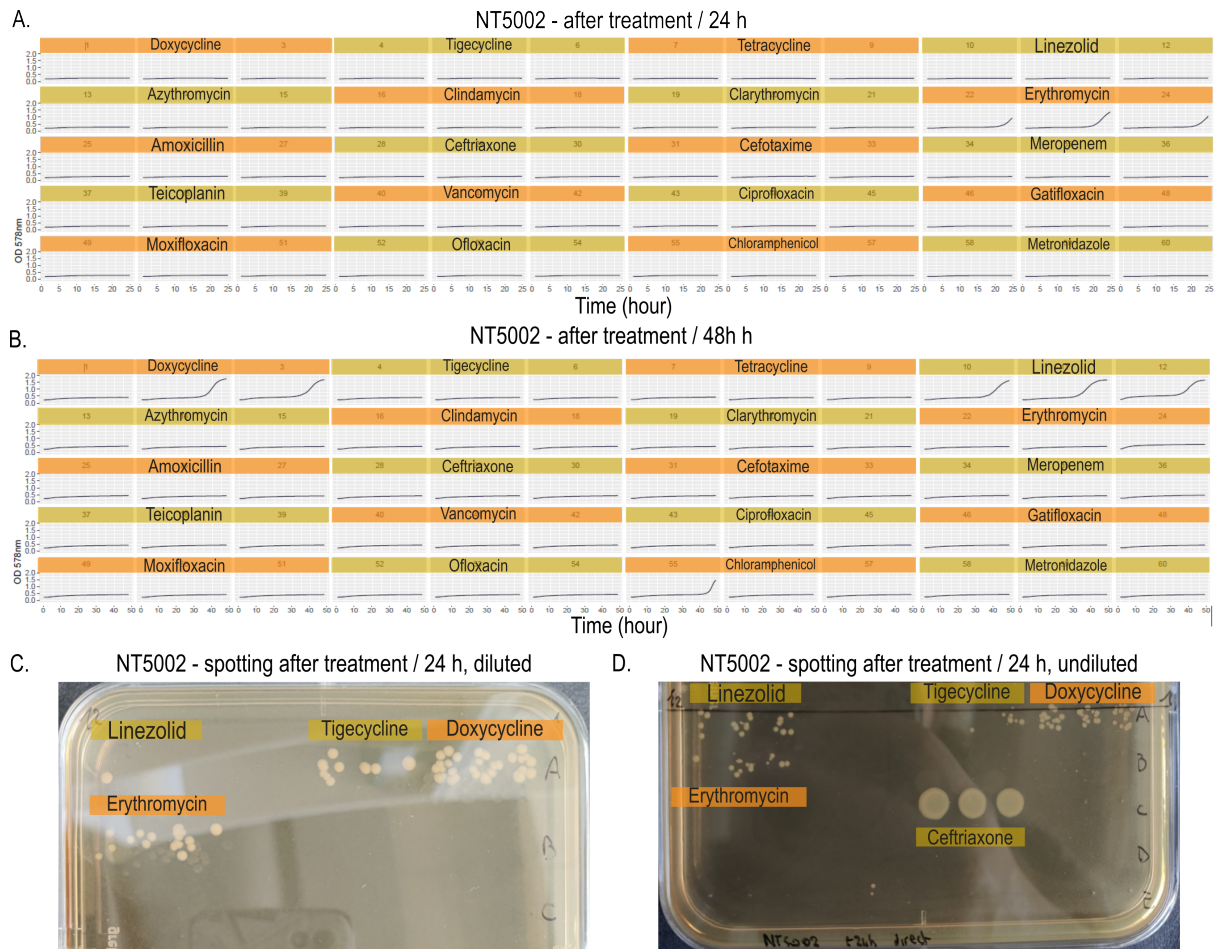


Figure 7.6. **A.** Read of bacterial growth for 24h after antibiotic treatment. **B.** Read of bacterial growth for 48h after a 24h antibiotic treatment. **C.** Spotting 3 μ L of the analysed strain after 24h treatment after a 1:20 dilution in PBS, as per the detection time method to see discrepancies between the two methodologies, a lower cell count can be seen, resulting in a lack of growth in the triplicates. **D.** Growth seen with ceftriaxone is due to a pipetting error, resulting in the use of an aliquot of antibiotic below the MIC. (*B. uniformis*), NT5002.

7.4 Survival assay with spotting

Although the previous method is working, the cell count is too low for detection due to a too high dilution, therefore, survival after antibiotic treatment will be calculated by counting spotted [CFU/mL] of each strain. The goal of this experiment is to determine the static-cidal activity of antibiotics against each strain. By counting the number of CFU present per mL, we can obtain the number of bacterial cells. Dividing the number of [CFU/mL] after 24h treatment, by the number of [CFU/mL] in no treatment (t0), we can determine a $<$ or $\geq 3 - \log_{10}$ CFU/mL reduction, and classify antibiotics respectively as bacteriostatic or bactericidal.

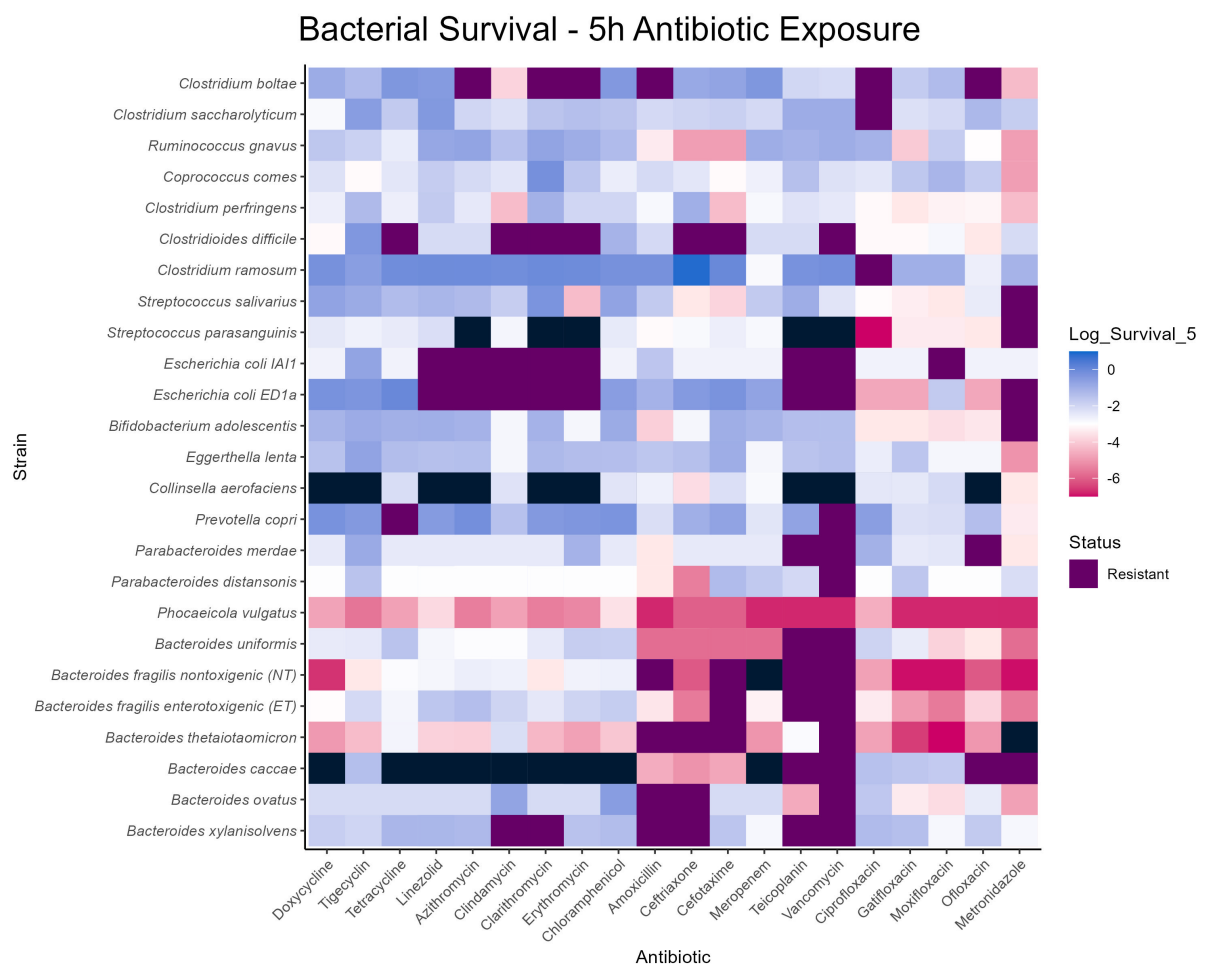


Figure 7.7. Heatmap of survival of strains of interest, after a treatment of 5h in mGAM with antibiotic at 5x MIC. Survival is represented on a log scale, with bacteriostatic effects of antibiotics in blue and bactericidal in red. Antibiotics are considered bactericidal at Log value -3 (white). Black tiles indicate values that couldn't be computed; this is due to spots with too many colonies present and not countable, thus static-cidal relationship cannot be inferred. Tiles of strains resistant to the antibiotic are highlighted in purple.

Spotting at a 5h timepoint can provide with more useful information on when a bactericidal effect can start to be seen. To determine the static-cidal activity, the definition indicates a reduction after a 24h treatment.

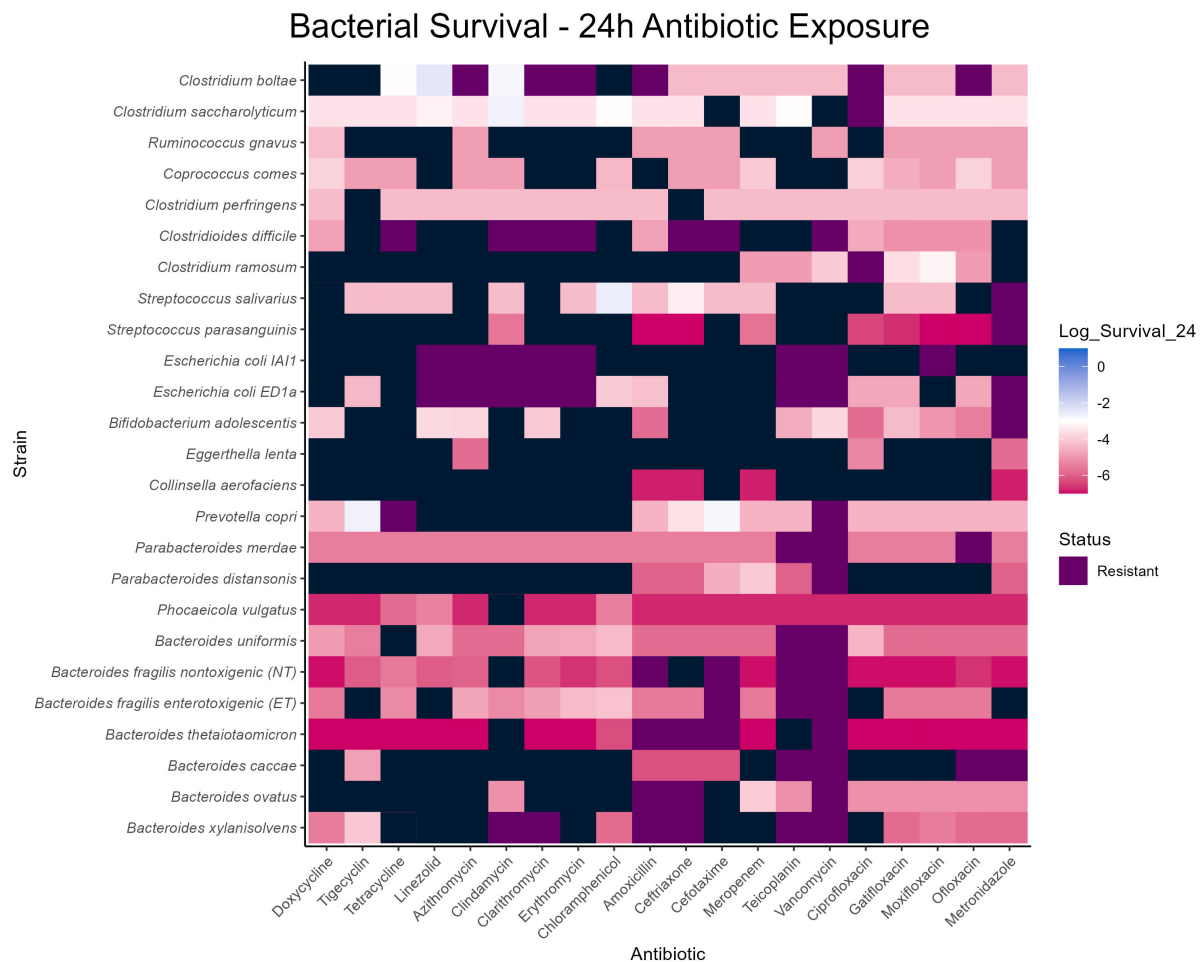


Figure 7.8. Heatmap of survivability of strains of interest, after a treatment of 24h in mGAM with antibiotic at 5x MIC. Purple tiles indicate the resistance of the strain towards antibiotics. Black tiles indicate values that couldn't be computed due once again too much growth, and are thus countable, thus static-cidal relationship cannot be inferred.

Discussion 8

8.1 MIC measurements

The heatmap shown in **figure 7.2** provides valuable data on the MIC of each antibiotic against 25 strains commonly found in the gut microbiota. This information is important given the lack of data on commensals on public databases such as EUCAST. From the data, we can see patterns in sensitivity or resistance depending on the phylogeny.

Regarding *Bacteroides* strains, literature shows it is expected to find higher levels of resistance, or lower rates of sensitivity, to antibiotics falling into the category of penicillins and cephalosporins in the beta-lactam group, [Rong et al., 2021]. This is the case for analysed strains such as *B. fragilis*, *B. thetaiotaomicron*, *B. xylanisolvens* which present a lower sensitivity to these antibiotics, resulting in higher values of MIC (**figure 7.2**).

Antibiotics in the glycopeptide category, such as vancomycin and teicoplanin, are usually deployed against Gram-positive bacteria, targeting cell wall synthesis, as previously explained in the **1.4.1** section. The presence of an Outer Membrane (OM) layer in Gram-negative bacteria prevents the passage of large molecules. Bacteroidetes are naturally more resistant to glycopeptides. This is generally seen in the case of strains such as *P. copri*, *P. merdae*, *P. distansonis*, *P. vulgatus*, *B. uniformis*, *B. fragilis (NT)*, *B. fragilis (ET)*, *B. thetaiotaomicron*, *B. caccae*, *B. ovatus*, and *B. xylanisolvens*. Vancomycin and teicoplanin are also used to treat *C. difficile* recurring infection [Al-Jashaami and DuPont, 2016], although the strain used in this study shows resistance, even at the high concentration of 625 mg/mL.

In all *Bacteroidetes*, the heatmap shows a lower sensitivity to beta-lactams such as penicillins and cephalosporins, with the exception of meropenem, a carbapenem whose small structure allows it to pass through the OM and affect the cell wall synthesis of gram negatives.

Regarding metronidazole, although strains such as *E. coli*, *S. sanguinis*, and *S. salivarius* are facultative anaerobes, the testing was performed in a strict anaerobic environment at levels of 0 ppm of oxygen. Therefore, these strains could present an intrinsic resistance to the compound,

generally attributed to a set of enzymes that are able to avoid the production of nitroso-radicals or may be able to neutralise them.

Regarding *E. coli*, macrolides such as erythromycin and azithromycin, are compounds to which the strain is considered intrinsically resistant, due to the large nature of the molecules.

Lower sensitivity to linezolid was less expected: some studies claim that bacteria resistant to the previously indicated PSIs-50s could be attributed more to resistance to linezolid due to the probable shared PTC binding site between this group of antibiotics [Diekema and Jones, 2000; Azzouz and Preuss, 2024]. Although linezolid is considered to have limited efficacy and not recommended for Gram-negative bacteria, especially *in vitro*, the vast majority of our analysed strains were effectively inhibited by it.

It is important to highlight that the effect of an antibiotic as static-cidal is not determined by the value of MIC. As an example, doxycycline shows in the heatmap a generally a lower MIC than chloramphenicol in *Bacteroidetes*, but this does not make it more effective in killing or inhibiting bacteria. In **table 8.1**, a summary of the theoretical expected results of sensitivities depending on the antibiotic.

Antibiotic	Gram +	Gram -	Anaerobic	Static-Cidal
Tetracycline	Yes	Yes	Yes	Bacteriostatic
Doxycycline	Yes	Yes	Yes	Bacteriostatic
Tigecycline	Yes	Yes	Yes	Bacteriostatic
Linezolid	Yes	Limited	Species-dependent	Bacteriostatic
Azithromycin	Yes	Limited	Species-dependent	Bacteriostatic
Clindamycin	Yes	Yes	G-	Bacteriostatic
Clarithromycin	Yes	Limited	Species-dependent	Bacteriostatic
Erythromycin	Yes	Limited	Species-dependent	Bacteriostatic
Amoxicillin	Yes	Species-dependent	Limited	Bactericidal
Ceftriaxone	Yes	Species-dependent	Limited	Bactericidal
Cefotaxime	Yes	Species-dependent	Limited	Bactericidal
Meropenem	Yes	Yes	Yes	Bactericidal
Teicoplanin	Yes	No	G+	Bactericidal
Vancomycin	Yes	No	G+	Bactericidal
Ciprofloxacin	Yes	Yes	Species-dependent	Bactericidal
Gatifloxacin	Yes	Yes	Species-dependent	Bactericidal
Moxifloxacin	Yes	Yes	Species-dependent	Bactericidal
Ofloxacin	Yes	Yes	Species-dependent	Bactericidal
Chloramphenicol	Yes	Yes	Yes	Bacteriostatic
Metronidazole			Yes	Bactericidal

Table 8.1. Summary of the theoretical general effects of antibiotics towards different types of bacteria; highlighted in green, all bacteriostatic antibiotics.

These patterns can be seen once the strains of interest are organised on their phylogenic relations. It is important to note that a lower MIC value of an antibiotic compared to another does not necessarily equate to higher effectiveness.

8.2 Survival Assay through detection time counting

To calculate survivability, the detection time, or the amount of time needed for the reader to detect cells and see growth, is needed.

Due to a low cell count, we weren't able to obtain the detection time after the 24h treatment for the majority of strains. Therefore, it was not possible to use this method to obtain results on the static-cidal relationship between strains and antibiotics. Further improvements of the method will be needed before implementing it in a high-throughput screen. This could be done by working with the totality of cells, separating them from the antibiotics through centrifugation, and resuspension in fresh media before proceeding with the read.

8.3 Survival Assay through Spotting

To determine the static-cidal relation between gut strains and antibiotics, a survival assay was performed at time-point 5h and time-point 24h. An antibiotic is determined to be bactericidal if the proportion between the CFU/mL count at time 24h and time 0h presents a reduction of 99.9% bacteria. Regrowth is possible after the 24h treatment, even if using a theoretically bactericidal antibiotic. Bacteria are treated at 5x the MIC to ensure that we are above the inhibiting/killing effect. The heatmap presented in **figure 7.7** and **figure 7.8**, shows in blue bacteriostatic effects, while in red bactericidal effects. Bacterial strains are ordered in phylogeny.

Black tiles indicate uncountable spottings in the experiment: we cannot infer any result regarding the antibiotic activity; further repetitions of the experiment, with serial dilutions for the 24h time point, will be needed for strains that have an uncountable number of CFUs in the spotting.

For bacterial strains like *Eggerthella lenta*(NT5024), almost no killing effect is visible for both bacteriostatic and bactericidal drugs. Most of these antibiotics' mechanisms of action target processes tied to bacterial growth: being *E. lenta* a slow-to-grow strain, the slow growth may affect the interaction with the antibiotic and its mechanism of action, resulting in a stasis during the treatment, and growth when inoculated in an antibiotic-free medium. This can affect the assay, leading to more uncountable spottings and lack of results.

Regarding the 5h time-point of antibiotic treatment, shown in **figure 7.7**, the majority of the analysed antibiotics at this time present bacteriostatic properties, given the short time-frame of the treatment. Different antibiotics from different classes of compounds will have different kinetics, bringing a sufficient reduction later in time. White tiles indicate antibiotics that are bactericidal, or almost (around $\log 2.9$). This highlights the need of a treatment long enough to leave time to the antibiotic to exert its effect.

Bactericidal effects can be seen in non-PSI antibiotics, against the majority of strains in the *Bacteroidetes* phylum. More noticeably, *P. vulgatus* is killed by all tested antibiotics early into the treatment, even PSIs, classically defined as bacteriostatic. Similarly *B. thetaiotaomicron* has low survivability against the majority of antibiotics.

Being *P. vulgatus* an ubiquitous bacterium strain, found in high abundance and frequently in different hosts [Rigottier-Gois et al., 2003], while also being one of the first colonisers in infants [Nilsen et al., 2023], the effects of these antibiotics could have noticeable health-related issues.

After a treatment of 24h with antibiotics, the available data as shown in **figure 7.8**, display the bactericidal activity of all PSIs, against the classical bacteriostatic definition, except for resistant strains towards specific antibiotics, highlighted in purple. No pattern is present that underlines an antibiotic working better than another: susceptibility towards the antibiotic is species-dependent.

Fluoroquinolones, which block DNA synthesis, and metronidazole, which produces free radicals, are the antibiotics that were able to kill more efficiently bacteria: this is probably tied to their mechanism of actions.

Bacteroidetes phylum, had the majority of strains affected. In the available data, all antibiotics, PSIs included, showed bactericidal effects; this proves that the usage, at least *in vitro* of antibiotics will lead to death of commensal bacteria in our gut, regardless of their classification. Further testing *in vitro* and community assay will be needed to see if this effect will be maintained, with a follow-up of the same survival assays closer to *in vivo* systems.

Conclusion 9

In this study, through a comprehensive high-throughput MIC measurement of 25 gut bacterial strains against 20 antibiotics, we were able to define MIC values and susceptibility patterns, both expected and not, of our strains of interest. This also provided valuable insight and data on the sensitivity of commensal strains, with patterns depending on their similarity highlighted through a phylogenetic tree, whose MIC is not available in databases such as EUCAST, and is needed for following survival assays.

To complement MIC measurements, we were able to develop a liquid culture detection time survival assay by comparing the shift in "lag" phase between t0 and t24h of each strain, translated in a CFU/mL concentration through building calibration curves. Although the methodology works, further optimisation is needed before implementing it into a high-throughput survival assay.

Finally, we were able to determine the static-cidal effect of antibiotics towards our gut strains of interest through a classic survival assay through spotting, and determining bactericidal activity by a ≥ 99.9 % reduction of cell count, after a 5h and 24h treatment. Through this assay, we were able to confirm on available data, that PSI antibiotics traditionally defined as bacteriostatic, exerted bactericidal effects on the majority of our analysed gut strains at the 24h time-point, presenting different strain-dependent susceptibility.

Reflection 10

With this research, we were able to prove that the bacteriostatic/bactericidal division used to classify antibiotics is not so accurate. Bacteriostatic antibiotics showed a killing effect on more than half of the strains of interest, with a species-dependent effect.

This work aims to ultimately refine antibiotic selection for treatment against pathogens, taking into consideration gut commensal strains, to limit side effects such as dysbiosis.

Future studies will focus on improving the survival assay through the detection time method by either upscaling the total volume for each repetition of antibiotic plus overnight strain culture. This will be performed by maintaining the same proportions to have a higher base cell count. Another method could be separating the antibiotic from the cells through centrifugation and resuspension. This will also allow to take a closer look and extend the study to more challenging to grow bacteria and more strains of interest.

In addition, the study will be further investigated by performing a survival assay, on bacterial communities both *in vitro*, and in more biologically relevant systems, such as intestinal organoids. This will be performed at clinically relevant concentrations of the previously studied antibiotics of interest, to expand upon their bactericidal effect on the beneficial gut microbiota strain, and further simulate the Host-Microbiota interactions and the protection that the mucus layer provides.

Bibliography

- Al-Jashaami and DuPont, 2016.** Layth S Al-Jashaami and Herbert L DuPont. *Management of Clostridium difficile infection*. Gastroenterology & hepatology, 12(10), 609, 2016.
- Aldred et al., 2014.** Katie J. Aldred, Robert J. Kerns and Neil Osheroff. *Mechanism of Quinolone Action and Resistance*. Biochemistry, 53(10), 1565–1574, 2014. doi: 10.1021/bi5000564. URL <https://doi.org/10.1021/bi5000564>. PMID: 24576155.
- Alonso and Guarner, 2013.** Virginia Robles Alonso and Francisco Guarner. *Linking the gut microbiota to human health*. British Journal of Nutrition, 109(S2), S21–S26, 2013.
- Andrews, 2001.** Jennifer M. Andrews. *Determination of minimum inhibitory concentrations*. Journal of Antimicrobial Chemotherapy, 48, 5–16, 2001. doi: 10.1093/jac/48.suppl_1.5.
- Angela Azzouz and Charles V Preuss. Linezolid. In *StatPearls [Internet]*. StatPearls Publishing, 2024.
- bio.libretexts.org, 2024.** bio.libretexts.org. *Clinical Microbiology Lab Manual*, 2024. URL https://bio.libretexts.org/Workbench/Clinical_Microbiology_Lab_Manual/19%3A_Chemical_Control_of_Microbial_Growth.
- Blondeau, 2004.** Joseph M Blondeau. *Fluoroquinolones: mechanism of action, classification, and development of resistance*. Survey of ophthalmology, 49(2), S73–S78, 2004.
- Bush and Bradford, 2016.** Karen Bush and Patricia A Bradford. *β -Lactams and β -lactamase inhibitors: an overview*. Cold Spring Harbor perspectives in medicine, 6(8), a025247, 2016.
- Chopra and Roberts, 2001.** Ian Chopra and Marilyn Roberts. *Tetracycline antibiotics: mode of action, applications, molecular biology, and epidemiology of bacterial resistance*. Microbiology and molecular biology reviews, 65(2), 232–260, 2001.
- Clemente et al., 2012.** Jose C Clemente, Luke K Ursell, Laura Wegener Parfrey and Rob Knight. *The impact of the gut microbiota on human health: an integrative view*. Cell, 148(6), 1258–1270, 2012.

- Collin et al., 2011.** Frédéric Collin, Shantanu Karkare and Anthony Maxwell. *Exploiting bacterial DNA gyrase as a drug target: current state and perspectives*. Applied microbiology and biotechnology, 92, 479–497, 2011.
- Corrêa-Oliveira et al., 2016.** Renan Corrêa-Oliveira, José Luís Fachi, Aline Vieira, Fabio Takeo Sato and Marco Aurélio R Vinolo. *Regulation of immune cell function by short-chain fatty acids*. Clinical & translational immunology, 5(4), e73, 2016.
- DeGruttola et al., 2016.** Arianna K DeGruttola, Daren Low, Atsushi Mizoguchi and Emiko Mizoguchi. *Current understanding of dysbiosis in disease in human and animal models*. Inflammatory bowel diseases, 22(5), 1137–1150, 2016.
- Diekema and Jones, 2000.** Daniel J Diekema and Ronald N Jones. *Oxazolidinones: a review*. Drugs, 59(1), 7–16, 2000.
- Donadio and Sosio, 2014.** Stefano Donadio and Margherita Sosio. *Inhibitors of Cell-Wall Synthesis*. Targets, Mechanisms and Resistance, 2014.
- Donohoe et al., 2011.** Dallas R Donohoe, Nikhil Garge, Xinxin Zhang, Wei Sun, Thomas M O’Connell, Maureen K Bunger and Scott J Bultman. *The microbiome and butyrate regulate energy metabolism and autophagy in the mammalian colon*. Cell metabolism, 13(5), 517–526, 2011.
- Edwards, 1993.** David I Edwards. *Nitroimidazole drugs-action and resistance mechanisms I. Mechanism of action*. Journal of Antimicrobial Chemotherapy, 31(1), 9–20, 1993.
- French, 2006.** GL French. *Bactericidal agents in the treatment of MRSA infections—the potential role of daptomycin*. Journal of Antimicrobial Chemotherapy, 58(6), 1107–1117, 2006.
- Gomaa, 2020.** Eman Zakaria Gomaa. *Human gut microbiota/microbiome in health and diseases: a review*. Antonie Van Leeuwenhoek, 113(12), 2019–2040, 2020.
- Tom A Hall et al., 1999.** Tom A Hall et al. BioEdit: a user-friendly biological sequence alignment editor and analysis program for Windows 95/98/NT. In *Nucleic acids symposium series*, number 41, 1, pages 95–98. Oxford, 1999.
- Higgins et al., 2003.** Paul G. Higgins, A. C. Fluit and F. J. Schmitz. *Fluoroquinolones: Structure and Target Sites*. Current drug targets, 4(2), 181–190, 2003.

- Horrocks et al., 2023.** Victoria Horrocks, Olivia G King, Alexander YG Yip, Inês Melo Marques and Julie AK McDonald. *Role of the gut microbiota in nutrient competition and protection against intestinal pathogen colonization*. Microbiology, 169(8), 001377, 2023.
- Hossain, 2024.** Tanim Jabid Hossain. *Methods for screening and evaluation of antimicrobial activity: A review of protocols, advantages, and limitations*. European Journal of Microbiology and Immunology, 14(2), 97–115, 2024.
- Hou et al., 2022.** Kaijian Hou, Zhuo-Xun Wu, Xuan-Yu Chen, Jing-Quan Wang, Dongya Zhang, Chuanxing Xiao, Dan Zhu, Jagadish B Koya, Liuya Wei, Jilin Li et al. *Microbiota in health and diseases*. Signal transduction and targeted therapy, 7(1), 1–28, 2022.
- Jandhyala et al., 2015.** Sai Manasa Jandhyala, Rupjyoti Talukdar, Chivkula Subramanyam, Harish Vuyyuru, Mitnala Sasikala and D Nageshwar Reddy. *Role of the normal gut microbiota*. World journal of gastroenterology: WJG, 21(29), 8787, 2015.
- Kapoor et al., 2017.** Garima Kapoor, Saurabh Saigal and Ashok Elongavan. *Action and resistance mechanisms of antibiotics: A guide for clinicians*. Journal of Anaesthesiology Clinical Pharmacology, 33(3), 300–305, 2017.
- Kennedy and Chang, 2020.** Megan S Kennedy and Eugene B Chang. *The microbiome: Composition and locations*. Progress in molecular biology and translational science, 176, 1–42, 2020.
- KONG et al., 2010.** KOK-FAI KONG, Lisa Schneper and Kalai Mathee. *Beta-lactam antibiotics: from antibiosis to resistance and bacteriology*. Apmis, 118(1), 1–36, 2010.
- Konstantinidis et al., 2020.** Theocharis Konstantinidis, Christina Tsigalou, Alexandros Karvelas, Elisavet Stavropoulou, Chrissoula Voidarou and Eugenia Bezirtzoglou. *Effects of antibiotics upon the gut microbiome: a review of the literature*. Biomedicines, 8(11), 502, 2020.
- Kos et al., 2008.** Blaženka Kos, Senka Džidić and Jagoda Šušković. *Antibiotic Resistance Mechanisms in Bacteria: Biochemical and Genetic Aspects*. Food technology and biotechnology, 46(1), 11–21, 2008.
- Kowalska-Krochmal and Dudek-Wicher, 2021.** Beata Kowalska-Krochmal and Ruth Dudek-Wicher. *The minimum inhibitory concentration of antibiotics: Methods, interpretation, clinical relevance*. Pathogens, 10(2), 165, 2021.

- LeBlanc et al., 2013.** Jean Guy LeBlanc, Christian Milani, Graciela Savoy De Giori, Fernando Sesma, Douwe Van Sinderen and Marco Ventura. *Bacteria as vitamin suppliers to their host: a gut microbiota perspective*. Current opinion in biotechnology, 24(2), 160–168, 2013.
- Madigan et al., 2014.** M.T. Madigan, J.M. Martinko, K.S. Bender, D.H. Buckley and D.A. Stahl. *Brock Biology of Microorganisms*. Always learning. Pearson, 2014. URL <https://books.google.ch/books?id=i1wPngEACAAJ>.
- Maier et al., 2018.** Lisa Maier, Mihaela Pruteanu, Michael Kuhn, Georg Zeller, Anja Telzerow, Exene Erin Anderson, Ana Rita Brochado, Keith Conrad Fernandez, Hitomi Dose, Hirotada Mori et al. *Extensive impact of non-antibiotic drugs on human gut bacteria*. Nature, 555(7698), 623–628, 2018.
- Maier et al., 2021.** Lisa Maier, Camille V Goemans, Jakob Wirbel, Michael Kuhn, Claudia Eberl, Mihaela Pruteanu, Patrick Müller, Sarela Garcia-Santamarina, Elisabetta Cacace, Boyao Zhang et al. *Unravelling the collateral damage of antibiotics on gut bacteria*. Nature, 599(7883), 120–124, 2021.
- Marano et al., 2023.** Giuseppe Marano, Marianna Mazza, Francesco Maria Lisci, Michele Ciliberto, Gianandrea Traversi, Georgios Demetrios Kotzalidis, Domenico De Berardis, Lucrezia Laterza, Gabriele Sani, Antonio Gasbarrini et al. *The Microbiota–Gut–Brain Axis: Psychoneuroimmunological Insights*. Nutrients, 15(6), 1496, 2023.
- Patrick B Murphy, Karlyle G Bistas, Preeti Patel and Jacqueline K Le. Clindamycin. In *StatPearls [Internet]*. StatPearls Publishing, 2024.
- National Center for Biotechnology Information, 2025a.** National Center for Biotechnology Information. *PubChem Compound Summary for CID 54671203, Doxycycline*, 2025a. URL <https://pubchem.ncbi.nlm.nih.gov/compound/Doxycycline>. Retrieved March 17, 2025.
- National Center for Biotechnology Information, 2025b.** National Center for Biotechnology Information. *PubChem Compound Summary for CID 5959, Chloramphenicol*, 2025b. URL <https://pubchem.ncbi.nlm.nih.gov/compound/Chloramphenicol>. Retrieved March 14, 2025.
- National Center for Biotechnology Information, 2025c.** National Center for Biotechnology Information. *PubChem Compound Summary for CID 446598, Clindamycin*,

2025c. URL <https://pubchem.ncbi.nlm.nih.gov/compound/Clindamycin>. Retrieved March 14, 2025.

National Center for Biotechnology Information, 2025d. National Center for Biotechnology Information. *PubChem Compound Summary for CID 441401, Linezolid*, 2025d. URL <https://pubchem.ncbi.nlm.nih.gov/compound/Linezolid>. Retrieved March 14, 2025.

Nemeth et al., 2014. Johannes Nemeth, Gabriela Oesch and Stefan P. Kuster. *Bacteriostatic versus bactericidal antibiotics for patients with serious bacterial infections: systematic review and meta-analysis*. Journal of Antimicrobial Chemotherapy, 70(2), 382–395, 2014. doi: 10.1093/jac/dku379.

Nilsen et al., 2023. Morten Nilsen, Eva Maria Rehbinder, Karin C Lødrup Carlsen, Guttorm Haugen, Gunilla Hedlin, Christine Monceyron Jonassen, Madeleine-Emilie Killingstad, Björn Nordlund, Ida Ormaasen, Håvard O Skjerven et al. *A globally distributed Bacteroides caccae strain is the most prevalent mother-child shared Bacteroidaceae strain in a large Scandinavian cohort*. Applied and Environmental Microbiology, 89(7), e00789–23, 2023.

Ginny C Oong and Prasanna Tadi. Chloramphenicol. In *StatPearls [Internet]*. StatPearls Publishing, 2020.

Pankey and Sabath, 2004a. G. A. Pankey and L. D. Sabath. *Clinical Relevance of Bacteriostatic versus Bactericidal Mechanisms of Action in the Treatment of Gram-Positive Bacterial Infections*. Clinical Infectious Diseases, 38(6), 864–870, 2004a. doi: 10.1086/381972.

Pankey and Sabath, 2004b. G. A. Pankey and L. D. Sabath. *Clinical Relevance of Bacteriostatic versus Bactericidal Mechanisms of Action in the Treatment of Gram-Positive Bacterial Infections*. Clinical Infectious Diseases, 38(6), 864–870, 2004b. doi: 10.1086/381972.

Pant et al., 2023. Kishor Pant, Senthil K Venugopal, Maria J Lorenzo Pisarello and Sergio A Gradilone. *The role of gut microbiome-derived short chain fatty acid butyrate in hepatobiliary diseases*. The American Journal of Pathology, 2023.

Papp-Wallace et al., 2011. Krisztina M Papp-Wallace, Andrea Endimiani, Magdalena A Taracila and Robert A Bonomo. *Carbapenems: past, present, and future*. Antimicrobial agents and chemotherapy, 55(11), 4943–4960, 2011.

Parth H Patel and Muhammad F Hashmi. Macrolides. In *StatPearls [Internet]*. StatPearls Publishing, 2023.

- Patel and Parmar, Jan 2023.** R.S. Patel and M. Parmar. *Doxycycline Hyclate*. StatPearls Publishing, Treasure Island, FL, 2023. URL <https://www.ncbi.nlm.nih.gov/books/NBK555888/>. Updated 2023 May 22.
- Shivali Patel, Charles V Preuss and Fidelia Bernice. Vancomycin. In *StatPearls [Internet]*. StatPearls Publishing, 2017.
- Petersen and Round, 2014.** Charisse Petersen and June L Round. *Defining dysbiosis and its influence on host immunity and disease*. Cellular microbiology, 16(7), 1024–1033, 2014.
- Portik and Wiens, 2020.** Daniel M Portik and John J Wiens. *Do Alignment and Trimming Methods Matter for Phylogenomic (UCE) Analyses?* Systematic Biology, 70(3), 440–462, 2020. doi: 10.1093/sysbio/syaa064.
- R Core Team, 2021.** R Core Team. *R: A Language and Environment for Statistical Computing*. R Foundation for Statistical Computing, Vienna, Austria, 2021. URL <https://www.R-project.org/>.
- Reece et al., 1991.** Richard J. Reece, Anthony Maxwell and James C. Wang. *DNA Gyrase: Structure and Function*. Critical reviews in biochemistry and molecular biology, 26(3-4), 335–375, 1991.
- Reynolds, 1989a.** Peter E Reynolds. *Structure, biochemistry and mechanism of action of glycopeptide antibiotics*. European Journal of Clinical Microbiology and Infectious Diseases, 8, 943–950, 1989a.
- Reynolds, 1989b.** Peter E Reynolds. *Structure, biochemistry and mechanism of action of glycopeptide antibiotics*. European Journal of Clinical Microbiology and Infectious Diseases, 8, 943–950, 1989b.
- Rigottier-Gois et al., 2003.** Lionel Rigottier-Gois, Violaine Rochet, Nathalie Garrec, Antonia Suau and Joël Doré. *Enumeration of Bacteroides species in human faeces by fluorescent in situ hybridisation combined with flow cytometry using 16S rRNA probes*. Systematic and applied microbiology, 26(1), 110–118, 2003.
- Rong et al., 2021.** Sebastian Martin Michael Rong, Arne Christian Rodloff and Catalina-Suzana Stingu. *Diversity of antimicrobial resistance genes in Bacteroides and Parabacteroides strains isolated in Germany*. Journal of Global Antimicrobial Resistance, 24, 328–334, 2021.

- Saikia and Chetia, 2024.** Shyamalima Saikia and Pankaj Chetia. *Antibiotics: from mechanism of action to resistance and beyond*. Indian Journal of Microbiology, 64(3), 821–845, 2024.
- Sayers et al., 2022.** Eric W Sayers, Evan E Bolton, J Rodney Brister, Kathi Canese, Jessica Chan, Donald C Comeau, Ryan Connor, Kathryn Funk, Chris Kelly, Sunghwan Kim et al. *Database resources of the national center for biotechnology information*. Nucleic acids research, 50(D1), D20–D26, 2022.
- Schlünzen et al., 2001.** Frank Schlünzen, Raz Zarivach, Jörg Harms, Anat Bashan, Ante Tocilj, Renate Albrecht, Ada Yonath and François Franceschi. *Structural basis for the interaction of antibiotics with the peptidyl transferase centre in eubacteria*. Nature, 413 (6858), 814–821, 2001.
- Shapira, 2016.** Michael Shapira. *Gut microbiotas and host evolution: scaling up symbiosis*. Trends in ecology & evolution, 31(7), 539–549, 2016.
- Shin et al., 2023.** Yoonhwa Shin, Sunhee Han, Juhui Kwon, Songhyun Ju, Tae Gyu Choi, Insug Kang and Sung Soo Kim. *Roles of short-chain fatty acids in inflammatory bowel disease*. Nutrients, 15(20), 4466, 2023.
- Slingerland et al., 2017.** Ann E Slingerland, Zaker Schwabkey, Diana H Wiesnoski and Robert R Jenq. *Clinical evidence for the microbiome in inflammatory diseases*. Frontiers in immunology, 8, 400, 2017.
- Spížek and Řezanka, 2017.** Jaroslav Spížek and Tomáš Řezanka. *Lincosamides: Chemical structure, biosynthesis, mechanism of action, resistance, and applications*. Biochemical pharmacology, 133, 20–28, 2017.
- Sprouffske, 2020.** Kathleen Sprouffske. *growthcurver: Simple Metrics to Summarize Growth Curves*, 2020. URL <https://CRAN.R-project.org/package=growthcurver>. R package version 0.3.1.
- Stevenson et al., 2016.** Keiran Stevenson, Alexander F McVey, Ivan BN Clark, Peter S Swain and Teuta Pilizota. *General calibration of microbial growth in microplate readers*. Scientific reports, 6(1), 38828, 2016.
- Thompson et al., 1994.** Julie D Thompson, Desmond G Higgins and Toby J Gibson. *CLUSTAL W: improving the sensitivity of progressive multiple sequence alignment through*

sequence weighting, position-specific gap penalties and weight matrix choice. Nucleic acids research, 22(22), 4673–4680, 1994.

Van Bambeke and Tulkens, 2001. Françoise Van Bambeke and Paul M Tulkens.

Macrolides: pharmacokinetics and pharmacodynamics. International Journal of Antimicrobial Agents, 18, 17–23, 2001.

Connor B Weir and Jacqueline K Le. Metronidazole. In *StatPearls [Internet]*. StatPearls Publishing, 2019.

Wiegand et al., 2008. Irith Wiegand, Kai Hilpert and Robert EW Hancock. *Agar and broth dilution methods to determine the minimal inhibitory concentration (MIC) of antimicrobial substances*. Nature protocols, 3(2), 163–175, 2008.

Yaghoubi et al., 2022. Sajad Yaghoubi, Angelina Olegovna Zekiy, Marcela Krutova, Mehrdad Gholami, Ebrahim Kouhsari, Mohammad Sholeh, Zahra Ghafouri and Farajolah Maleki. *Tigecycline antibacterial activity, clinical effectiveness, and mechanisms and epidemiology of resistance: narrative review*. European Journal of Clinical Microbiology & Infectious Diseases, pages 1–20, 2022.

Yoneyama and Katsumata, 2006. Hiroshi Yoneyama and Ryoichi Katsumata. *Antibiotic resistance in bacteria and its future for novel antibiotic development*. Bioscience, biotechnology, and biochemistry, 70(5), 1060–1075, 2006.

Zaura et al., 2015. Egija Zaura, Bernd W. Brandt, M. Joost Teixeira de Mattos, Mark J. Buijs, Martien P. M. Caspers, Mamun-Ur Rashid, Andrej Weintraub, Carl Erik Nord, Ann Savell, Yanmin Hu, Antony R. Coates, Mike Hubank, David A. Spratt, Michael Wilson, Bart J. F. Keijser and Wim Crielaard. *Same Exposure but Two Radically Different Responses to Antibiotics: Resilience of the Salivary Microbiome versus Long-Term Microbial Shifts in Feces*. mBio, 6(6), 10.1128/mbio.01693–15, 2015. doi: 10.1128/mbio.01693-15. URL <https://journals.asm.org/doi/abs/10.1128/mbio.01693-15>.

11.1 Calibration curves

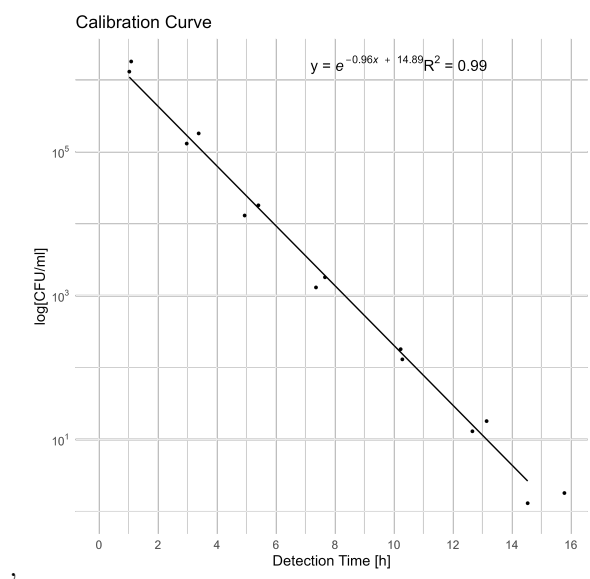


Figure 11.1. *Phocaeicola vulgatus*, NT5001, Slope: -0,9573706, Intercept: 14,88999893

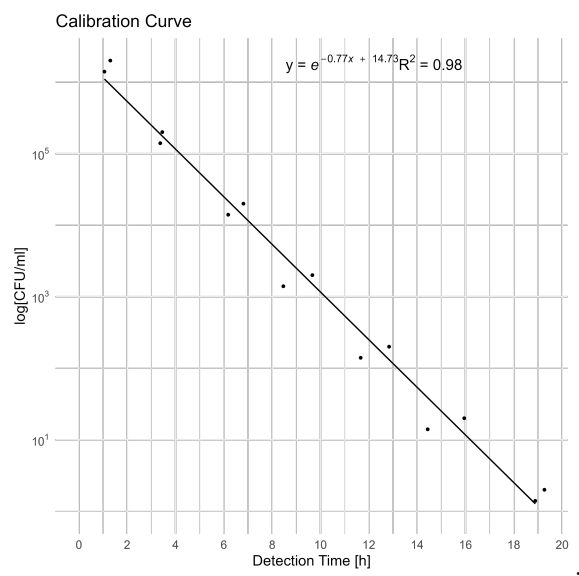


Figure 11.2. *Bacteroides uniformis*, NT5002, Slope: -0,76676182, Intercept: 14,72537799

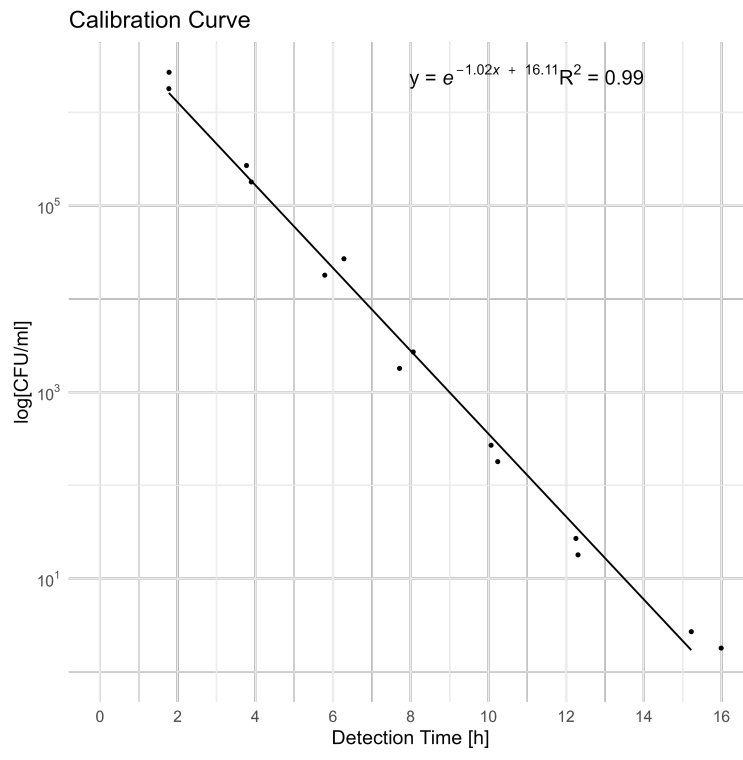


Figure 11.3. *Bacteroides fragilis nontoxigenic* (NT), NT5003, Slope: -1,023117918, Intercept: 16,11431257

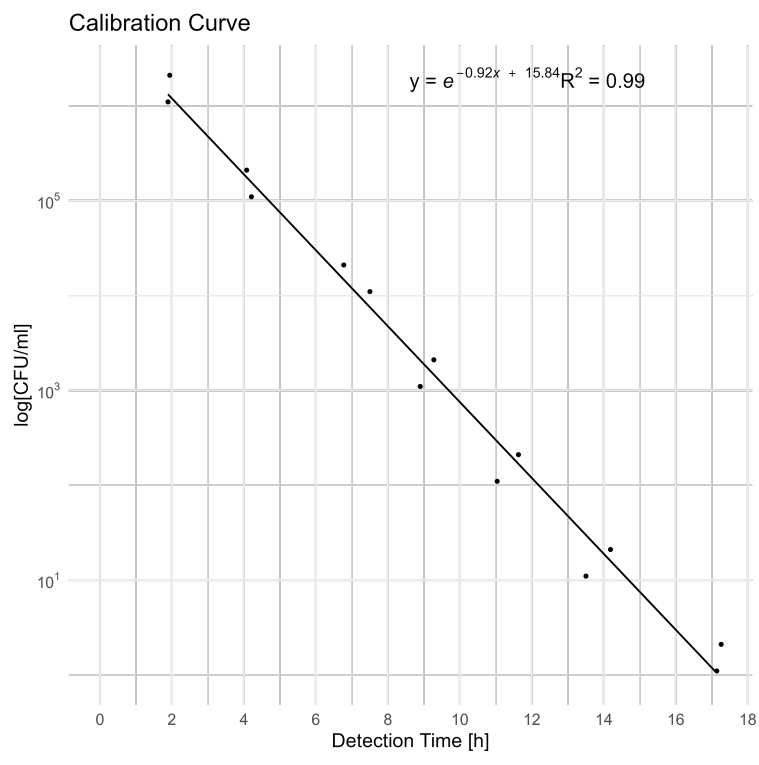


Figure 11.4. *Bacteroides thetaiotaomicron*, NT5004, Slope -0,921531978, Intercept: 15,8380799

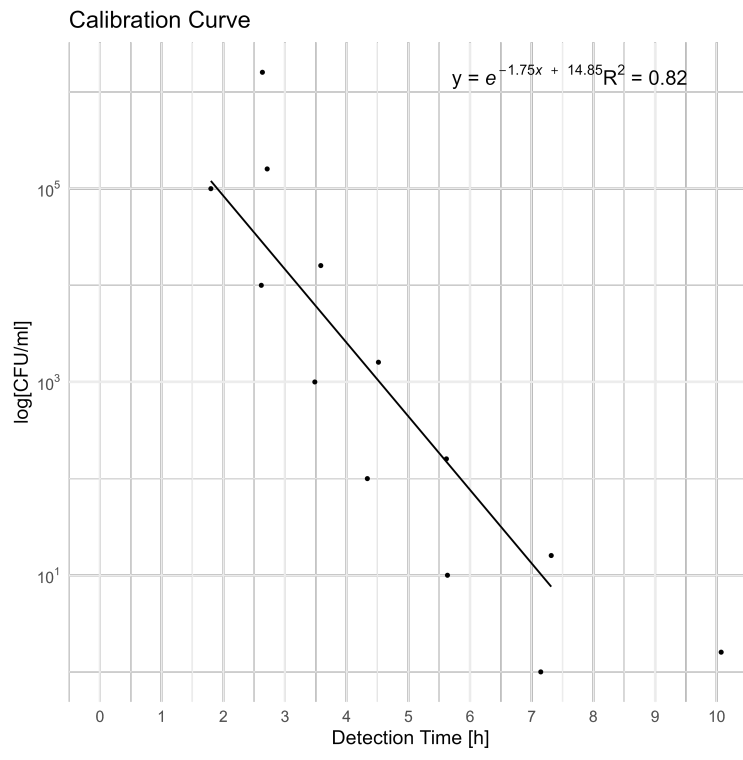


Figure 11.5. *Clostridium ramosum*, NT5006, Slope: -1,751733874, Intercept: 14,84752198

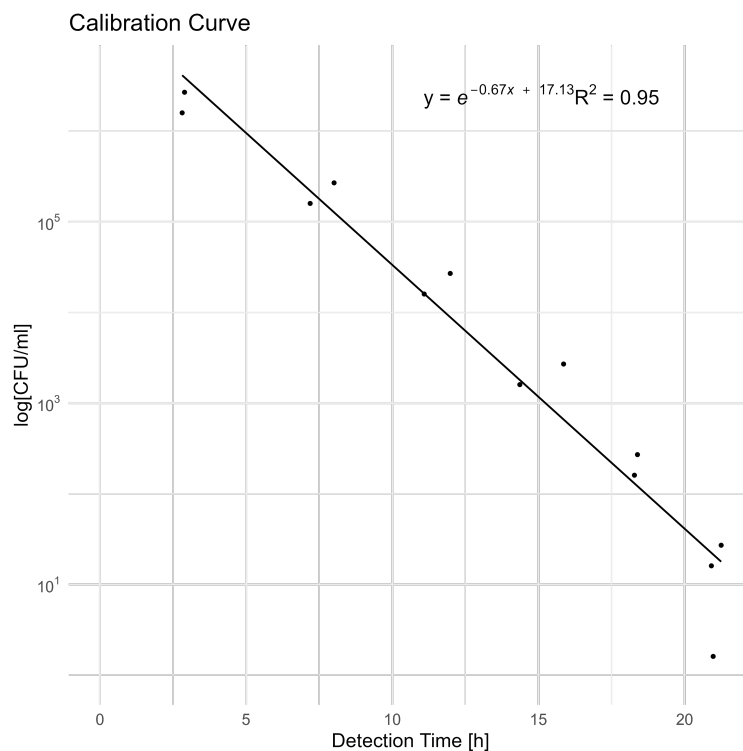


Figure 11.6. *Prevotella copri*, NT5019, Slope: -6,70535, Intercept: 17,13

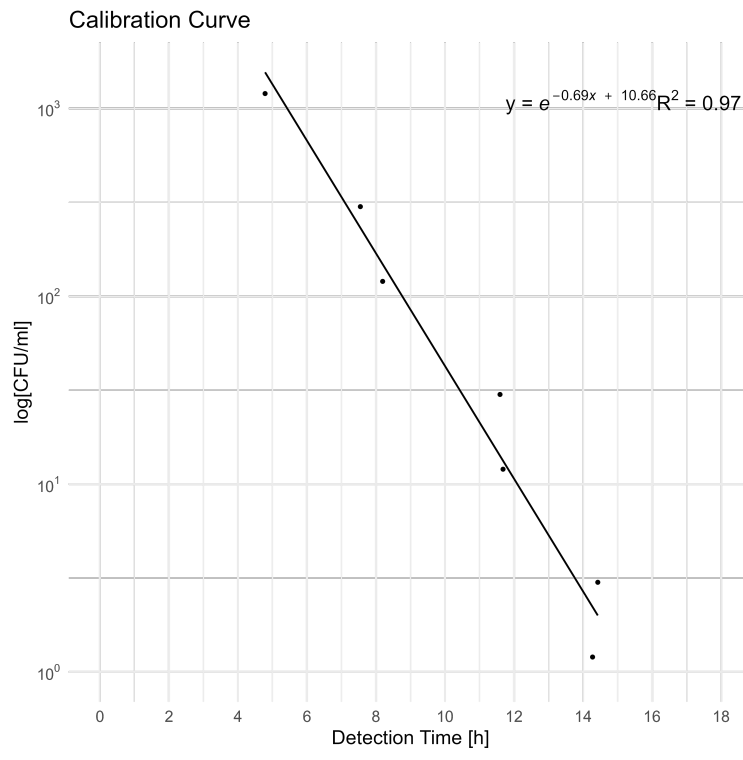


Figure 11.7. *Bifidobacterium adolescentis*, NT5022, Slope: -0,690699598, Intercept: 10,65668406

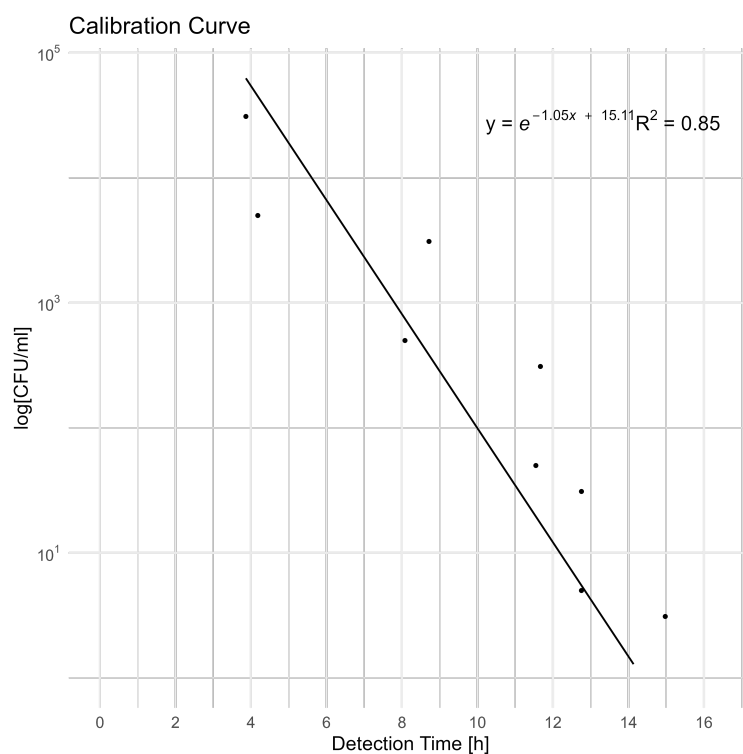


Figure 11.8. *Eggerthella lenta*, NT5024, Slope: -1,050959809, Intercept: 15,10823989

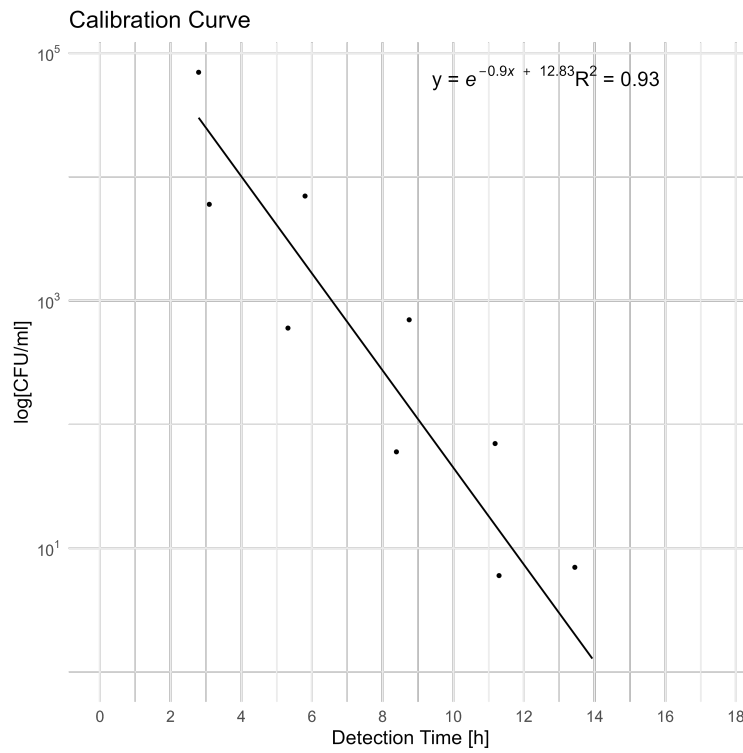


Figure 11.9. *Clostridium boltae*, NT5026, Slope: -0,903126258, Intercept: 12,833956

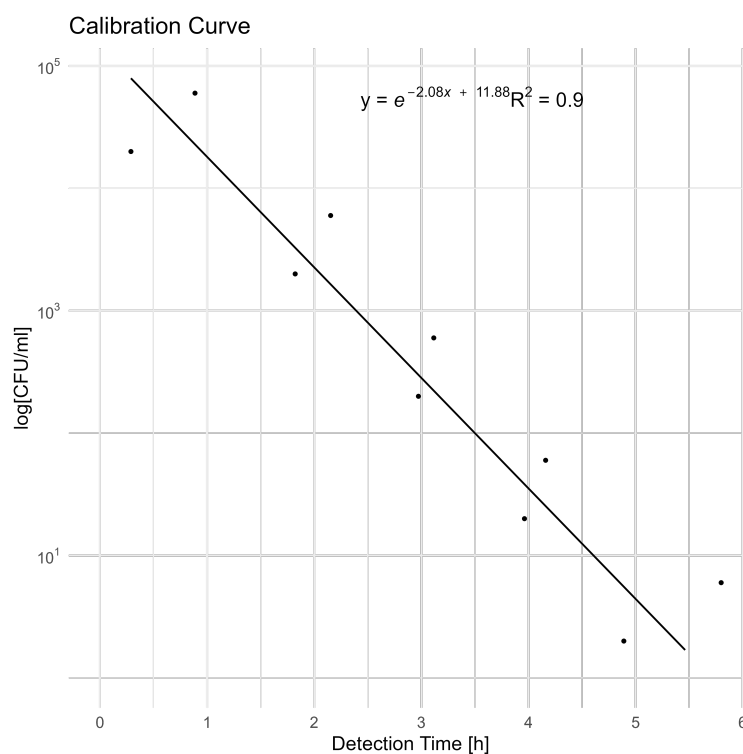


Figure 11.10. *Clostridium perfringens*, NT5032, Slope: -2,079193394, Intercept: 11,88345581

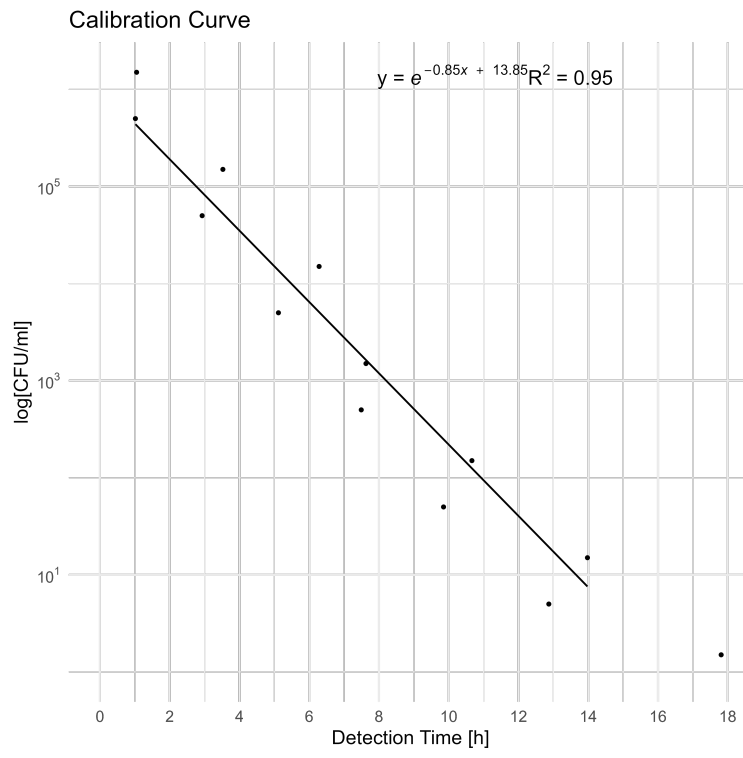


Figure 11.11. *Bacteroides fragilis enterotoxigenic (ET)*, NT5033, Slope: -0,845996952, Intercept: 13,85049836

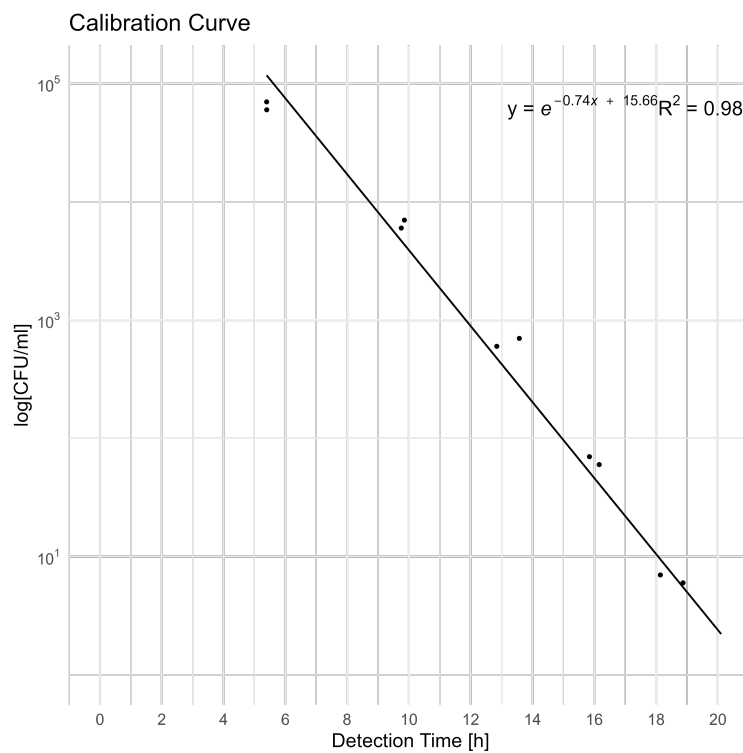


Figure 11.12. *Clostridium saccharolyticum*, NT5037, Slope: -0,739474587, Intercept: 15,66375174

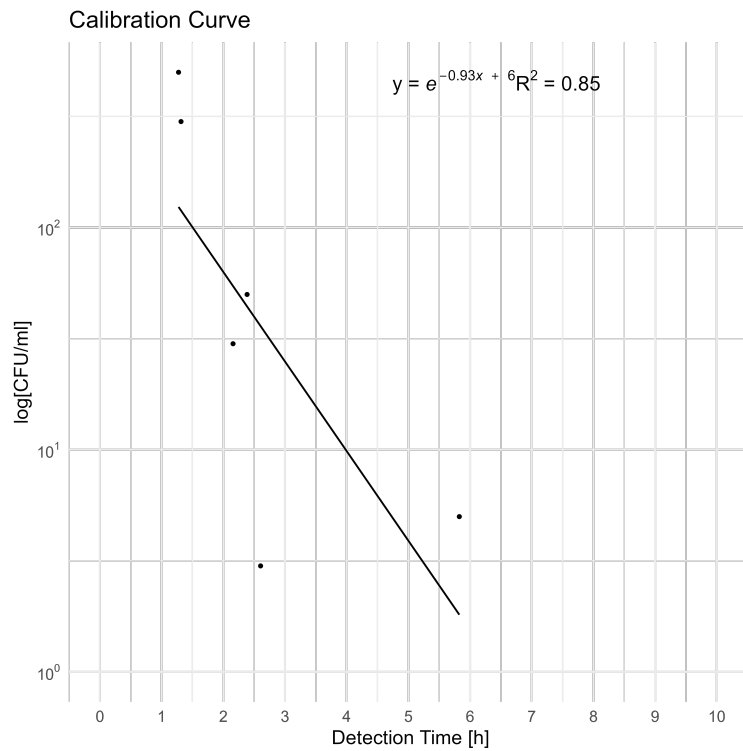


Figure 11.13. *Streptococcus salivarius*, NT5038, Slope: -0,928474606, Intercept: 6,002371126

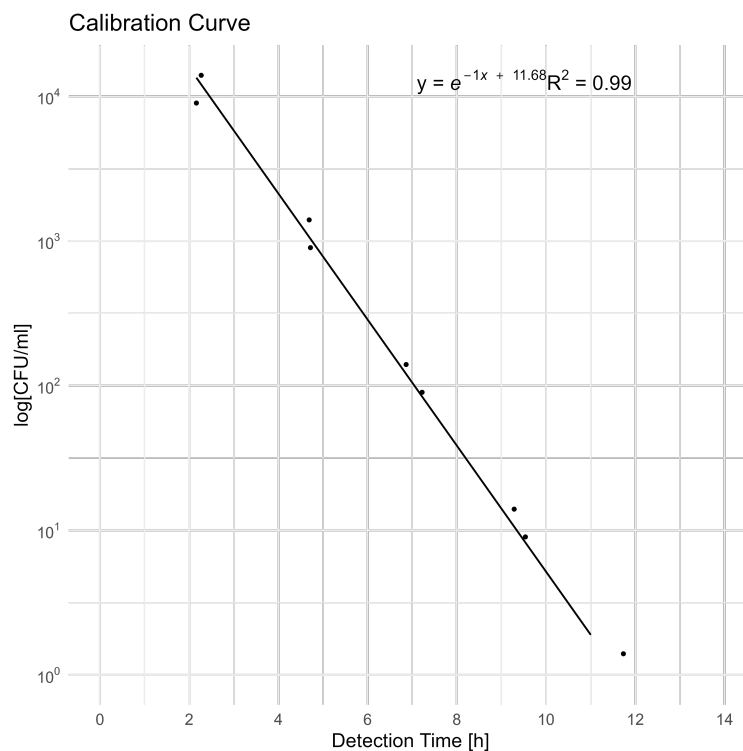


Figure 11.14. *Ruminococcus gnavus*, NT5046, Slope: -1,003417681, Intercept: 11,67834909

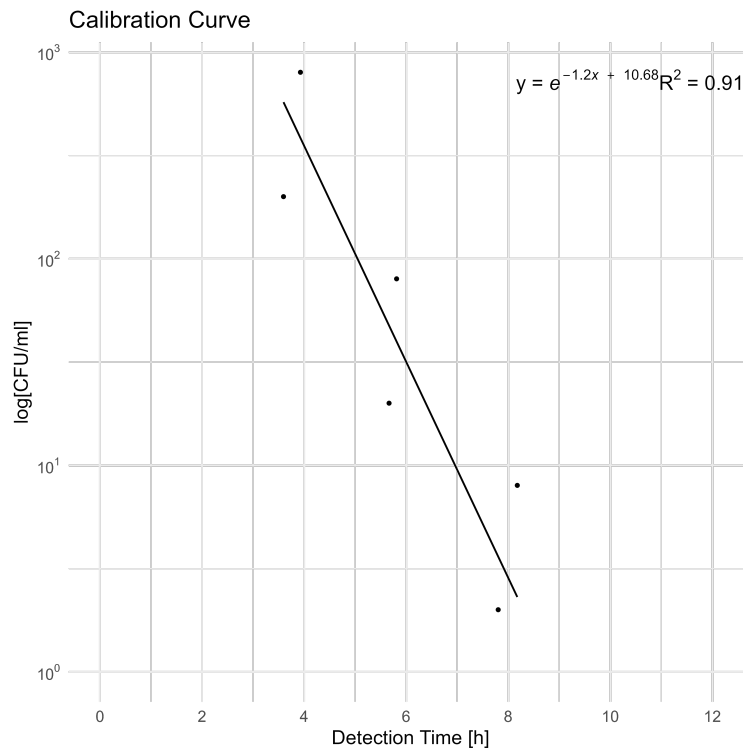


Figure 11.15. *Coprococcus comes*, NT5048, Slope: -1,204326032, Intercept: 10,68360622

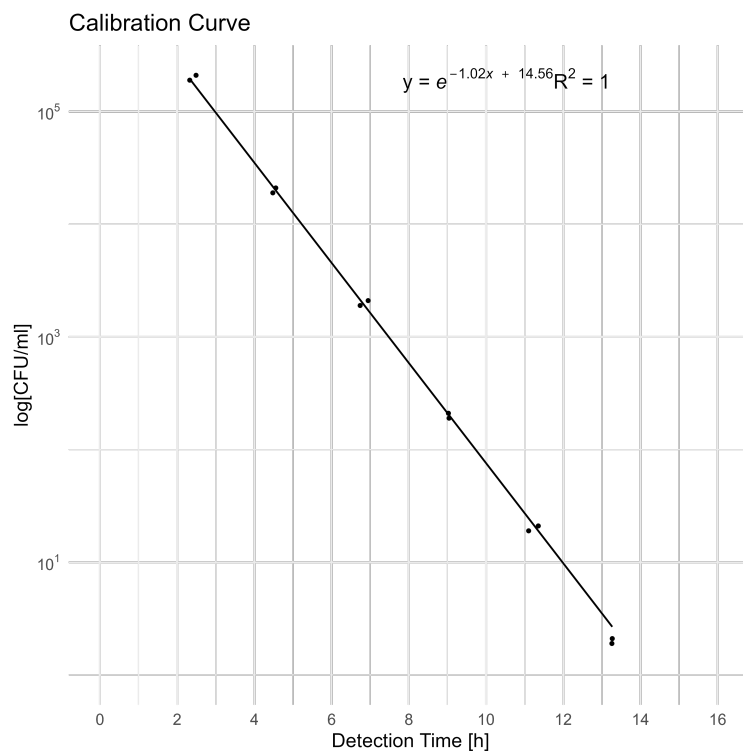


Figure 11.16. *Bacteroides caccae*, NT5050, Slope: -1,023319422, Intercept: 14,56141612

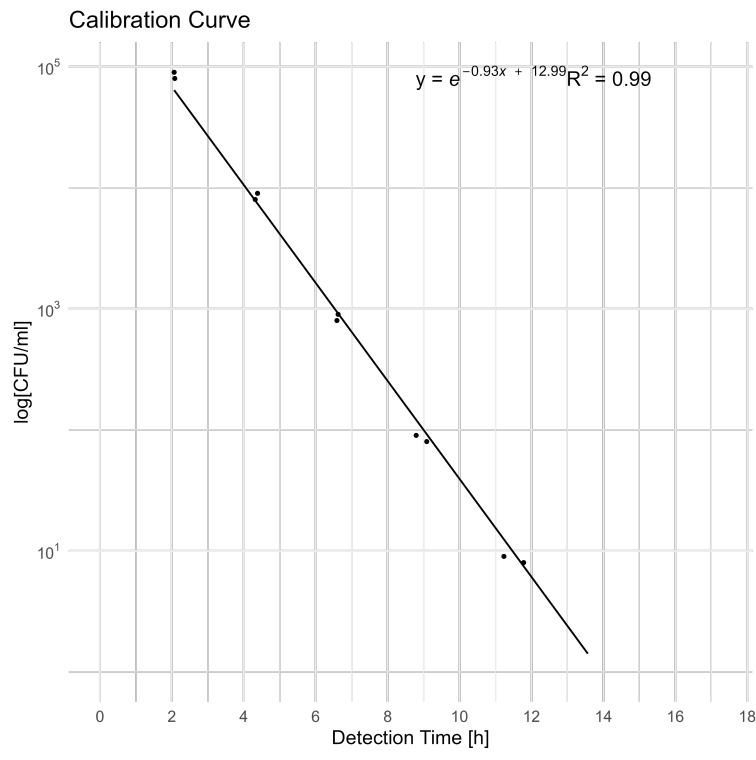


Figure 11.17. *Bacteroides ovatus*, NT5054, Slope: -0,932064098, Intercept: 12,99288366

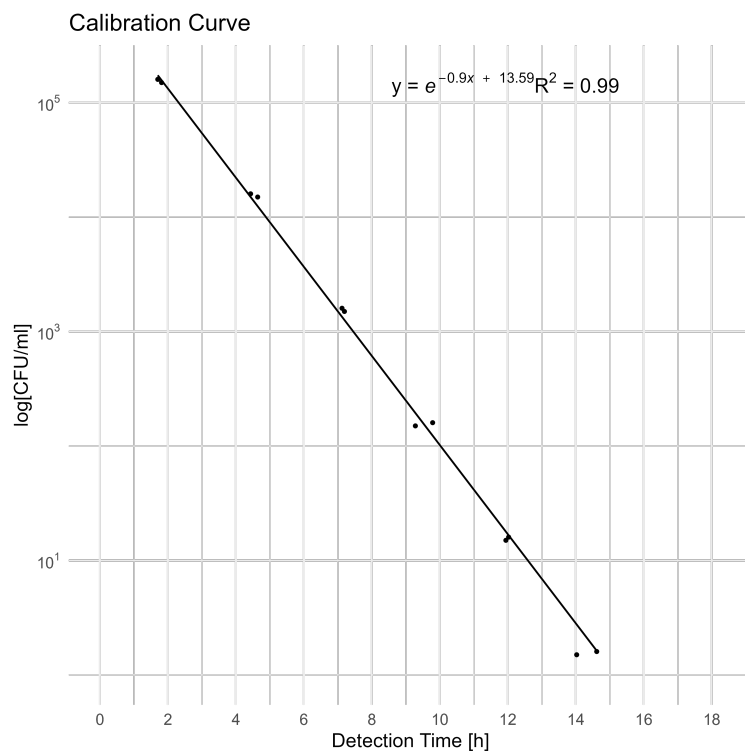


Figure 11.18. *Bacteroides xylanisolvens*, NT5064, Slope: -0,896832482, Intercept: 13,59201357

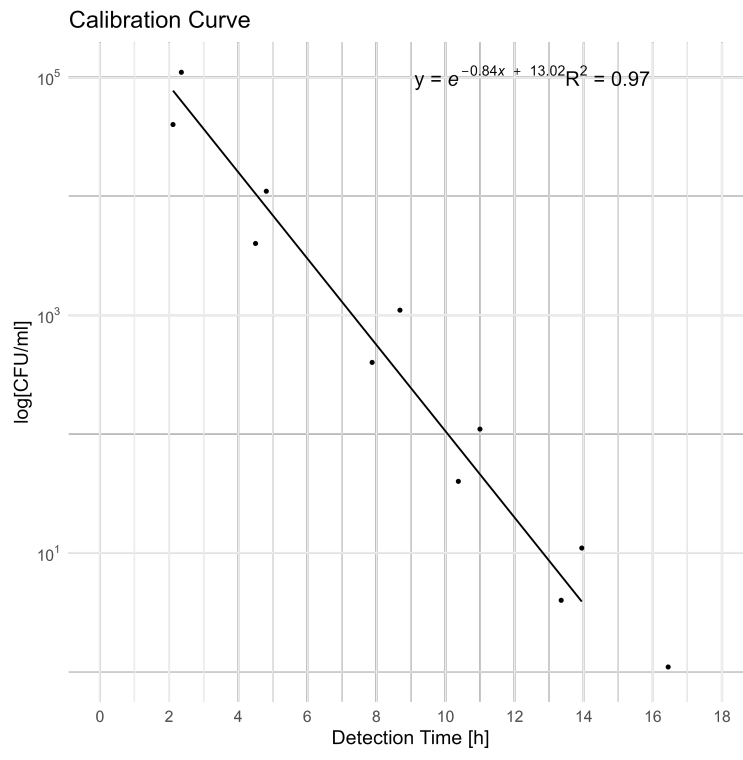


Figure 11.19. *Parabacteroides merdae*, NT5071, Slope: -0,574528569, Intercept: 9,572267313

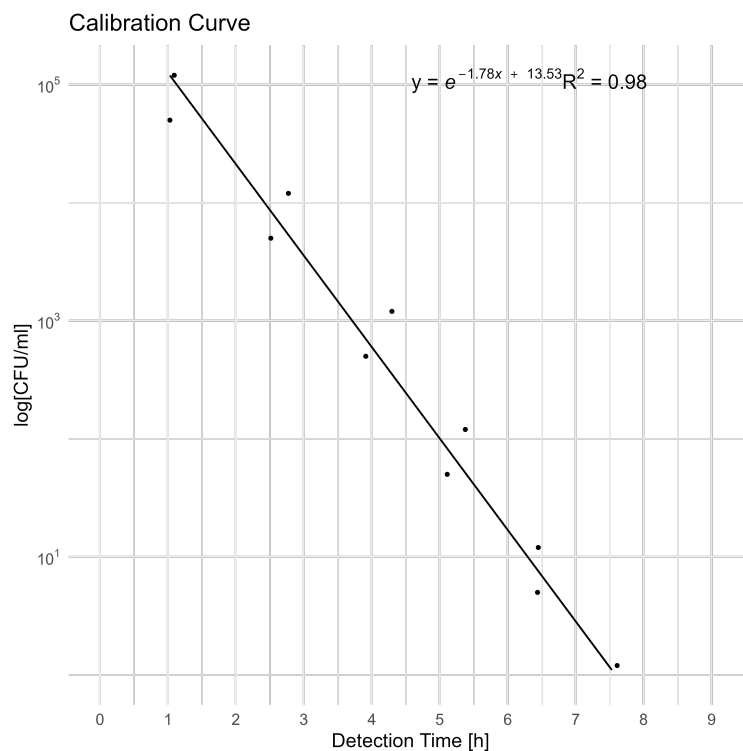


Figure 11.20. *Streptococcus parasanguinis*, NT5072, Slope: -1,783435424, Intercept: 13,52889483

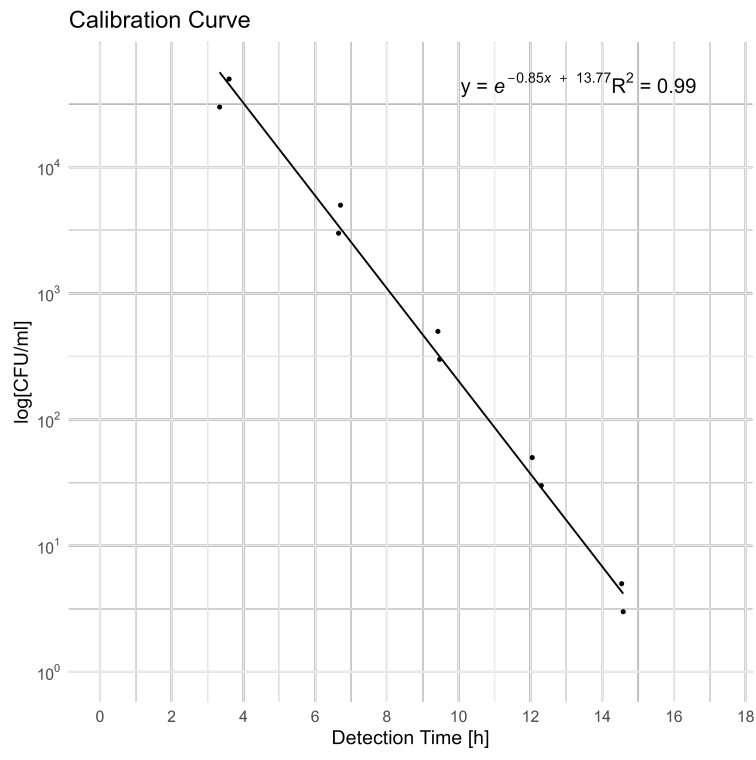


Figure 11.21. *Collinsella aerofaciens*, NT5073, Slope: -0,889466165, Intercept: 13,95486806

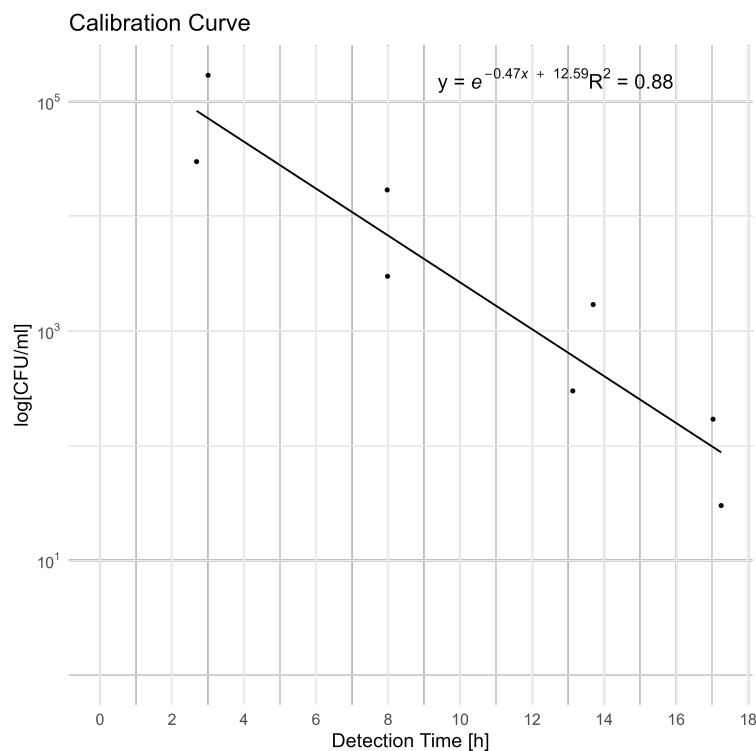


Figure 11.22. *Parabacteroides distasonis*, NT5074, Slope: -0,567641934, Intercept: 12,95664479

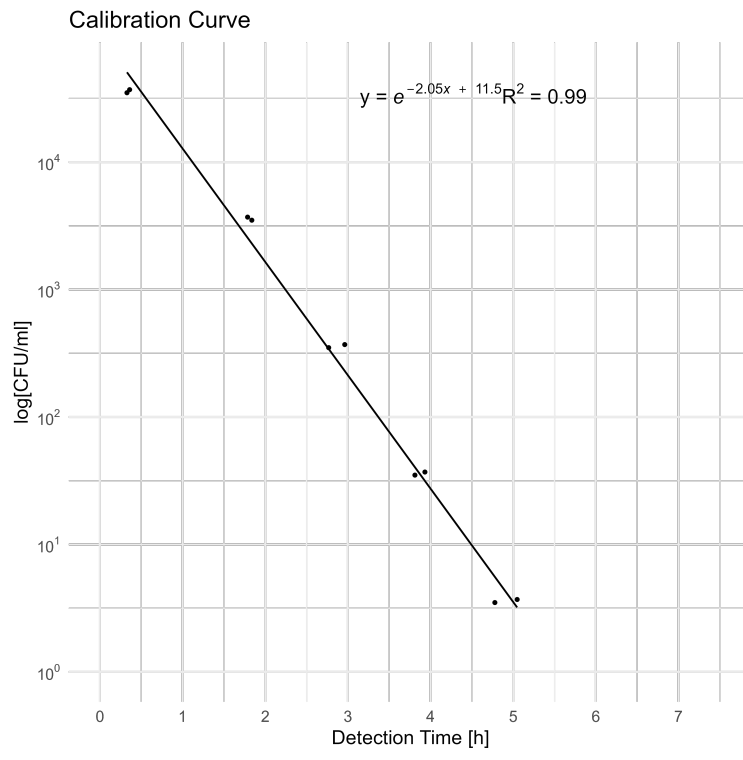


Figure 11.23. *Escherichia coli* IAI1, NT5077, Slope:-2,047929499, Intercept: 11,50298021

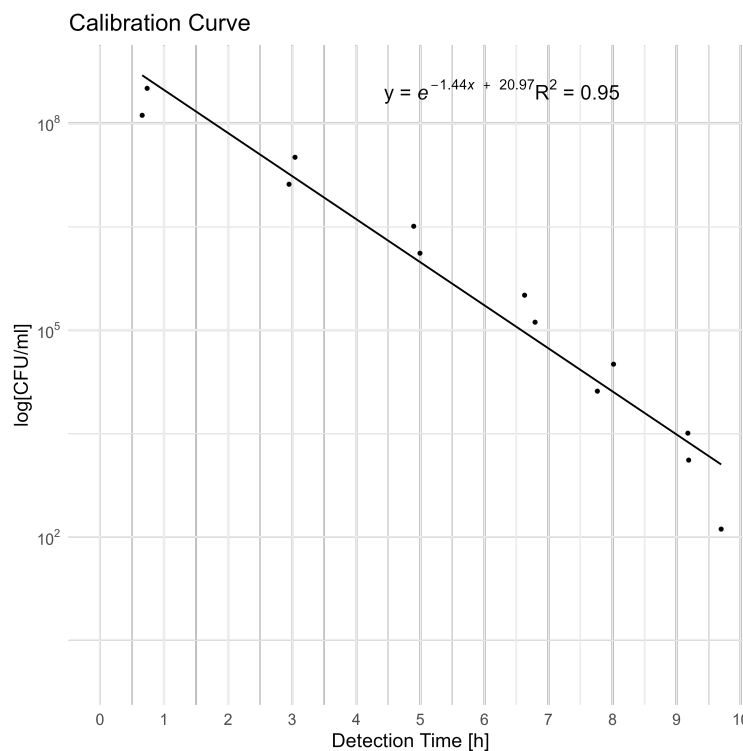


Figure 11.24. *Escherichia coli* ED1a, NT5078, Slope -1,437823684, Intercept: 20,96690874

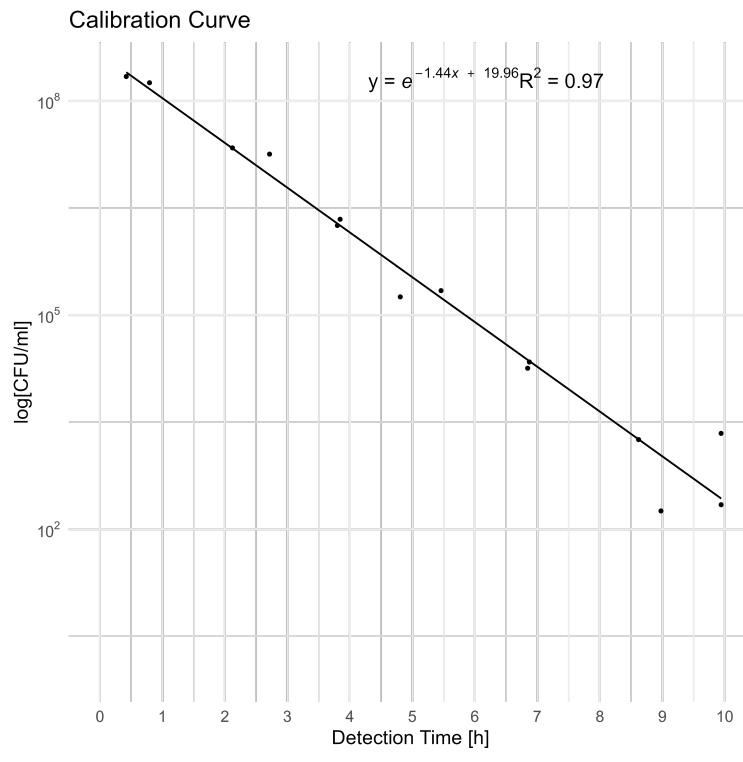


Figure 11.25. *Clostridioides difficile*, NT5083, Slope: -1,444451534, Intercept: 19,95568871